

# Late Holocene environmental conditions in Coronation Gulf, southwestern Canadian Arctic Archipelago: evidence from dinoflagellate cysts, other non-pollen palynomorphs, and pollen



ANNA J. PIEŃKOWSKI,<sup>1,\*†</sup> PETA J. MUDIE,<sup>2</sup> JOHN H. ENGLAND,<sup>1</sup> JOHN N. SMITH<sup>3</sup> and MARK F. A. FURZE<sup>4</sup>

<sup>1</sup>Department of Earth and Atmospheric Sciences, University of Alberta, Edmonton, Alberta, Canada

<sup>2</sup>Geological Survey of Canada – Atlantic, Dartmouth, Nova Scotia, Canada

<sup>3</sup>Department of Fisheries and Oceans, Bedford Institute of Oceanography, Dartmouth, Nova Scotia, Canada

<sup>4</sup>Earth and Planetary Science Division, Department of Physical Sciences, Grant MacEwan University, Edmonton, Alberta, Canada

Received 19 November 2010; Revised 22 February 2011; Accepted 27 February 2011

**ABSTRACT:** Boxcore 99LSSL-001 (68.095° N, 114.186° W; 211 m water depth) from Coronation Gulf represents the first decadal-scale marine palynology and late Holocene sediment record for the southwestern part of the Northwest Passage. The record was studied for organic-walled microfossils (dinoflagellate cysts, non-pollen palynomorphs), pollen, terrestrial spores, and sediment characteristics. <sup>210</sup>Pb, <sup>137</sup>Cs, and three accelerator mass spectrometry <sup>14</sup>C dates constrain the chronology. Three prominent palaeoenvironmental zones were identified. During the interval AD 1470–1680 (Zone I), the climate was warmer and wetter than at present, and environmental conditions were more favourable to biological activity and northward boreal forest migration, with reduced sea-ice and a longer open-water (growing) season. The interval AD 1680–1940 (Zone II) records sea-ice increase, and generally cool, polar conditions during the Little Ice Age. During AD 1940–2000 (Zone III), organic microfossils indicate an extended open-water season and decreased sea-ice, with suggested amelioration surpassing that of Zone I. Although more marine studies are needed to place this record into an appropriate context, the succession from ameliorated (Zone I) to cooler, sea-ice influenced conditions (Zone II) and finally to 20th-century warming (Zone III) corresponds well with several terrestrial climatic records from the neighbouring mainland and Victoria Island, and with lower-resolution marine records to the west. Copyright © 2011 John Wiley & Sons, Ltd.

**KEYWORDS:** sea-ice; environmental change; Northwest Passage; Little Ice Age; decadal scale.

## Introduction

Marine geological studies in the Canadian Arctic Archipelago (CAA) are in their infancy, in contrast to the wealth of Quaternary palaeoenvironmental data from over four decades of island-based work (e.g. Prest *et al.*, 1968; Dyke and Prest, 1987; Dyke *et al.*, 1996; Dyke, 2004; Smol *et al.*, 2005; England *et al.*, 2006, 2009). However, the extent of the intervening marine channels throughout this ~2.5 million km<sup>2</sup> area (Fig. 1a) emphasizes the need for marine sedimentary records. Only a few palaeoenvironmental studies extending to deglaciation are available from the archipelago channels and immediate environs (e.g. MacLean *et al.*, 1989; Levac *et al.*, 2001; Mudie *et al.*, 2006; Scott *et al.*, 2009; Vare *et al.*, 2009; Gregory *et al.*, 2010; Ledu *et al.*, 2010a, b; Pieńkowski *et al.*, 2011). Similarly, despite several studies emphasizing modern microfossil distributions (e.g. Vilks, 1969; Schröder-Adams *et al.*, 1990; Hunt and Corliss, 1993; Mudie and Rochon, 2001; Richerol *et al.*, 2008a), high-resolution late Holocene records from the CAA channels are rare. Here we present the first late Holocene (past ~530 years) decadal-scale record from Coronation Gulf, based on sedimentology, organic-walled microfossils (dinoflagellate cysts = dinocysts, other non-pollen palynomorphs = NPP), pollen, spores, and charcoal. Hitherto, the closest late Holocene studies were from Amundsen Gulf and the Beaufort Sea (Richerol *et al.*, 2008b; Schell *et al.*, 2008), and Dease and Victoria straits (Ledu *et al.*, 2010a; Belt *et al.*, 2010). However, complementary Holocene lacustrine records are available from Victoria Island (Peros and Gajewski, 2009; Porinchi *et al.*, 2009; Fortin and Gajewski, 2010) and

mainland Canada (Nichols, 1975; Zabenskie and Gajewski, 2007; MacDonald *et al.*, 2009; Peros and Gajewski, 2009).

Our marine record helps to contextualize modern and projected Arctic environmental shifts, including changes in sea level, sea-ice, ocean circulation, and ecosystems (Smol *et al.*, 2005; Solomon *et al.*, 2007; Turner *et al.*, 2007). Given the intrinsic marine–terrestrial linkages within the CAA (England, 1987), our new data are evaluated in the context of interrelated regional terrestrial and marine archives.

## Environmental setting

### Physiography and geology

The south coast of Coronation Gulf comprises the northwestern edge of the igneous (Precambrian) Canadian Shield. Neo-Proterozoic rocks are common throughout the area, with carbonates of the Arctic Platform underlying Dolphin and Union Strait and Victoria Island, and igneous rocks comprising island chains in Coronation Gulf (Thorsteinsson and Tozer, 1962; Kerr *et al.*, 1997). The south shore consists of cliffs dissected by river valleys, the coast becoming low and poorly drained around the Coppermine, Rae, and Richardson river deltas (Dredge, 2001). The north coast of the gulf exhibits prominent glacial landforms (moraines and streamlined landforms), rising to 120–300 m inland (Sharpe, 1992).

### Climate and vegetation

Low Arctic climate with long cold winters and short cool summers characterizes Coronation Gulf (Maxwell, 1981). At Kugluktuk, mean monthly air temperatures range from –32°C (for January) to +15°C July; average –10.6°C; minimum –47°C; maximum +35°C; Environment Canada, 2010a). Continuous permafrost underlies most of the region away

\*Correspondence: A. J. Pieńkowski, at †present address below.

E-mail: a.pienkowski@bangor.ac.uk

†Present address: School of Ocean Sciences, Bangor University, Menai Bridge, Anglesey, Wales, UK.

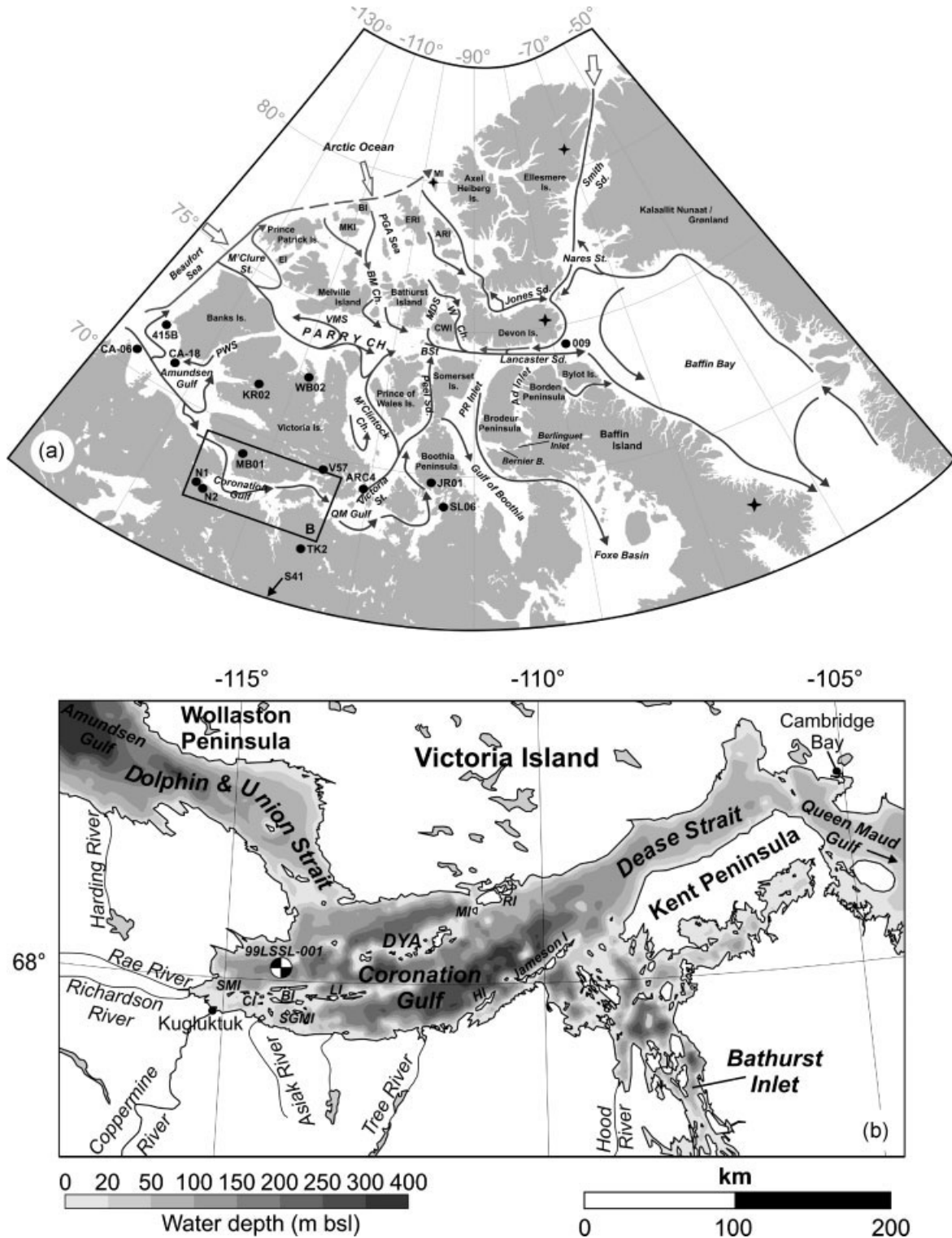


**Figure 1.** (a) Map of the Canadian Arctic Archipelago. The generalized modern surface circulation (indicated by arrowed lines) and regions of significant Arctic Ocean water input (marked by large arrows) are based on Ingram and Prinsenberg (1998). Regional (primarily lacustrine) studies from Victoria Island and the Canadian mainland referred to in the text are indicated by dots. Lake studies include: KR02 (Peros and Gajewski, 2008), WB02 (Fortin and Gajewski, 2010), MB01 and SL06 (Peros and Gajewski, 2009), V57 (Porinchiu *et al.*, 2009), JR01 (Zabenskie and Gajewski, 2007), S41 (MacDonald *et al.*, 2009), TK2 (Paul *et al.*, 2010). N1 and N2 refer to the peat sections studied by Nichols (1975) at Coppermine Beach and Saddleback Hill, respectively. The closest marine studies include Schell *et al.* (2008); cores 415B, CA-06, CA-18) and Belt *et al.* 2010 (ARC4). Core 009 is also shown (Ledu *et al.*, 2008; republished with additional data as Ledu *et al.*, 2010a, b). The core sites of Richerol *et al.* (2008b) are off the map in Mackenzie Trough. Abbreviations: ARI, Amund Ringnes Islands; BI, Borden Island; BM Ch., Byam Martin Channel; CWI, Cornwallis Island; EI, Eglington Island; ERI, Ellef Ringnes Island; MDS, McDougall Sound; MI, Meighen Island; MKI, Mackenzie King Island; PGA Sea, Prince Gustav Adolf Sea; PR Inlet, Prince Regent Inlet; PWS, Prince of Wales Strait; W Ch., Wellington Channel. Ice core records mentioned in the text are denoted by a star. (b) Detailed inset of Coronation Gulf, showing bathymetry (based on Jakobsson *et al.*, 2008) and 99LSSL-001 core site. Abbreviations: BI, Berens Islands; CI, Couper Islands; DYA, Duke of York Archipelago; HI, Hepburn Island; LI, Lawford Islands; MI, Murray Island; RI, Richardson Islands; SGM, Sir Graham Moore Islands; SMI, Seven Mile Island.

from the coast (Maxwell, 1981). Low Arctic tundra vegetation covers the mainland, except ~15 km inland from the Coppermine River delta/valley, where it is replaced by taiga woodland (CAVM Team, 2003). Tundra vegetation consists of heath dwarf birch (*Ericales*, *Betula nana*) communities with scattered herbs on drier soils. Tussock grasses (*Poaceae*), sedges (*Cyperaceae*, including cottongrass/*Eriophorum*), and mosses (*Bryales*, *Sphagnales*) grow on wetter terrain (CAVM Team, 2003). The taiga woodland ecozone encompasses scattered dwarf spruce trees (black and white spruce, *Picea mariana*, *P. glauca*), low thickets of willow (*Salix*), birches, alder (*Alnus*), with infrequent aspen and balsam poplars (*Populus* spp.). Mid to high Arctic tundra vegetation, including prostrate dwarf shrubs (*Betula nana*, *Salix*, *Dryas integrifolia*), sedges, herbs, and mosses cover southern Victoria Island (CAVM Team, 2003).

### Oceanography

Numerous large rivers (Rae, Richardson, Coppermine, Asiatic; Fig. 1b) drain into southern Coronation Gulf, with total annual freshwater inflow estimated at ~15% that of the Mackenzie River ( $10\,700\text{ m}^3\text{ s}^{-1}$ ). Mean annual Coppermine River flow is  $262\text{ m}^3\text{ s}^{-1}$  (peak  $1330\text{ m}^3\text{ s}^{-1}$ ), whereas smaller rivers show smaller flows (Tree River  $\sim 37\text{ m}^3\text{ s}^{-1}$ ; Hood River  $\sim 76\text{ m}^3\text{ s}^{-1}$ ; Environment Canada, 2010b). Arctic Ocean Surface Water enters Coronation Gulf ( $\sim 230 \times 100\text{ km}$ ; average depth  $\sim 150\text{ m}$ ; Fig. 1b) through Dolphin and Union Strait (Ingram and Prinsenberg, 1998), whose shallow sill (20–30 m) severely limits deep-water advection of Atlantic origin (Beaudoin *et al.*, 2004). Surface waters eventually reach Baffin Bay via Parry Channel (Fig. 1a; Ingram and Prinsenberg, 1998). August water temperature profiles in north-central Amundsen Gulf and northwest Coronation Gulf show a temperature of  $\sim 6^\circ\text{C}$  in the surface layer, decreasing rapidly to  $0^\circ\text{C}$  below 50 m depth. However, surface waters off the Coppermine River, close to our study site, are less saline (0–10 m:  $\sim 22$ ; >10 m:  $\sim 27$ ) than in Amundsen Gulf (0–200 m:  $\sim 23$ ; >200 m:  $\sim 34$ ; Beaudoin *et al.*, 2004). Eastern Coronation Gulf exhibits August salinities and temperatures of  $\sim 24$  and  $\sim 6^\circ\text{C}$  at the surface, which both decrease to  $\sim 28$  and  $-0.5^\circ\text{C}$  at 40 m. Deeper water (>190 m) is colder (below  $-1^\circ\text{C}$ ) and more saline (29; McLaughlin *et al.*, 2009). Landfast first-year ice dominates Coronation Gulf from mid October to July (Pharand, 1984), whereas multi-year ice is rare (Howell *et al.*, 2008). By early July, ice breaks up, assisted by river runoff. Open-water conditions prevail until freeze-up in mid October/November, consolidation occurring in December (Ingram and Prinsenberg, 1998). Historical data suggest significant reduction in sea-ice concentration since 1968 (Stewart *et al.*, 2007).

## Materials and methods

### Core materials

Boxcore 99LSSL-001 was retrieved from southwestern Coronation Gulf ( $68.095^\circ\text{N}$ ,  $114.186^\circ\text{W}$ ; Tundra Northwest research cruise, CCGS *Louis S. St-Laurent*, 1999) in a small, deep (211 m) basin 48 km NE of the Coppermine River mouth (Fig. 1b). Push cores taken from the boxcore were refrigerated onboard and in their repository at the Geological Survey of Canada – Atlantic, where they were later split and described (PJM; 2001–2004). The present study is based upon push cores 001E and 001F, showing an identical stratigraphy of 43–45 cm of massive clayey silt (Fig. 2) with a mottled brown surface layer. Smear slides were examined (001E; 5 cm intervals) for fine sand, and calcareous and siliceous microfossils prior to palynological processing.

### Sedimentological and geochemical analyses

Water content (%) was calculated from wet weight:dry weight ratios, corrected for a salinity of 29 (Noorany, 1984). Grain size (99LSSL-001E; 5 cm intervals) was measured using a Beckman Coulter LS230 laser diffraction instrument (size range 0.4–2000  $\mu\text{m}$ ). For carbon analysis, samples (5–10 g; 5 cm intervals, 99LSSL-001F) were oven-dried ( $60\text{--}65^\circ\text{C}$ ), powdered, digested in 10% hydrochloric acid, repeatedly rinsed with deionized water, oven-dried ( $60\text{--}65^\circ\text{C}$ ), and ground. 100 mg subsamples were subsequently analysed for total organic carbon (TOC) on a LECO CHN analyser (model #630-100-400) and values are presented as weight percentages.

### Chronostratigraphy

Core 99LSSL-001 chronology is constrained by  $^{210}\text{Pb}$  and  $^{137}\text{Cs}$  measurements, and four accelerator mass spectrometry (AMS) radiocarbon dates (Fig. 2, Table 1).  $^{210}\text{Pb}$  was measured by alpha counting of  $^{210}\text{Pb}$  electrodeposited onto nickel discs, while  $^{226}\text{Ra}$ -supported  $^{210}\text{Pb}$  levels were determined by Ge gamma ray detection (Smith and Walton, 1980).  $^{137}\text{Cs}$  was measured on dried samples using a hyper-pure Ge gamma ray detector (1 cm diameter well; Smith *et al.*, 2009). The recent sedimentation rate was calculated using a two-step process (Smith, 2001). Background  $^{210}\text{Pb}$  ( $^{226}\text{Ra}$ -supported) is given by the approach of  $^{210}\text{Pb}$  activities to a constant baseline value in the deeper core (independently confirmed by direct  $^{226}\text{Ra}$  measurements). Background-supported  $^{210}\text{Pb}$  ( $\approx 1\text{ dpm g}^{-1}$ ) was subtracted from total  $^{210}\text{Pb}$ , giving excess  $^{210}\text{Pb}$  ( $^{210}\text{Pb}_{\text{ex}}$ ). An average sedimentation rate ( $0.12\text{ cm a}^{-1}$ ) was calculated from the slope of a least squares exponential fit of  $^{210}\text{Pb}_{\text{ex}}$  as a function of sediment depth.  $^{137}\text{Cs}$  was plotted on the geochronological scale determined from the  $^{210}\text{Pb}$  sedimentation rate. Generally, the  $^{137}\text{Cs}$  threshold horizon should be in agreement with a  $^{210}\text{Pb}$  date of ca. AD 1952 corresponding to the first significant appearance of  $^{137}\text{Cs}$  in global sediments (US Pacific Ocean Tests). In core 99LSSL-001, the initial appearance of measurable  $^{137}\text{Cs}$  ( $>1.5\text{ Bq kg}^{-1}$ ) occurred at a  $^{210}\text{Pb}$  date of ca. AD 1950, suggesting minimal bioturbation. Nevertheless, some mixing cannot be ruled out and  $0.12\text{ cm a}^{-1}$  represents a maximum sedimentation rate (thus minimum ages) as bioturbation can mix  $^{210}\text{Pb}$  deeper into the core, diminishing the  $^{210}\text{Pb}$  gradient and giving the appearance of higher sedimentation rates. This  $^{210}\text{Pb}$  sedimentation rate is considered valid for the upper  $\sim 12\text{ cm}$  of the core, representing the first  $\sim 100\text{ a}$  of sediment deposition before the sampling year (AD 1999). At depths  $>100\text{ a}$ ,  $^{210}\text{Pb}_{\text{ex}}$  had decreased to levels undistinguishable from the  $^{226}\text{Ra}$ -supported background.

Radiocarbon dates on marine materials (Table 1) were calibrated using CALIB 6.0 (Stuiver *et al.*, 2010) based on Marine09 (Reimer *et al.*, 2009), incorporating a  $\Delta R$  of  $335 \pm 85\text{ a}$  for the CAA (Coulthard *et al.*, 2010). We report all dates in calibrated years AD. An age model was constructed by plotting minimum  $^{210}\text{Pb}$  ages, and three calibrated radiocarbon median probability ages (from CALIB 6.0) and their 1 and  $2\sigma$  ranges against core depth (Fig. 2). An envelope connecting  $2\sigma$  age limits of the three radiocarbon dates was defined, its lower margin being constrained by  $^{210}\text{Pb}$  minimum ages, and excluding the possibility of age reversals (Fig. 2). A conservative best-fit curve, as close to straight as the  $2\sigma$  envelope would permit, was then drawn, constituting our preferred age model. Errors are not given in the text, but are defined by the upper and lower limits of the  $2\sigma$  envelope. Beyond the deepest  $^{14}\text{C}$  date, a linear extrapolation was used. The organic marine polychaete worm tube  $^{14}\text{C}$  date (OS-79112, 19 cm; Table 1) was excluded from the age–depth model because it dated 310  $^{14}\text{C}$  a older than mollusc shell fragments from the same horizon (UCIAMS-

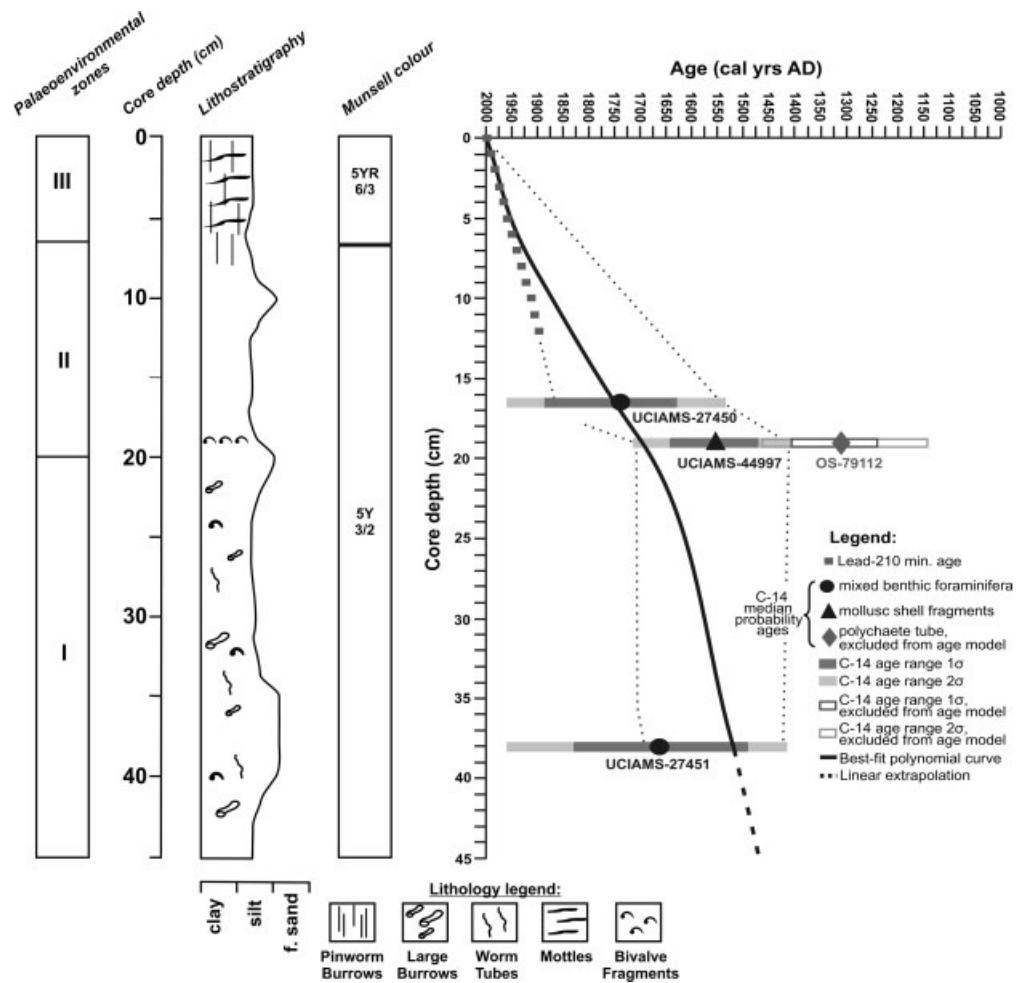


**Figure 2.** Lithology of core 99LSSL-001, based on a combination of adjacent push cores 001E and 001F. The age–depth model for core 99LSSL-001 is based on Pb measurements and <sup>14</sup>C dating. All radiocarbon dates were calibrated using CALIB 6.0 (Stuiver *et al.*, 2010) based on the marine calibration dataset Marine09 (Reimer *et al.*, 2009) and incorporating a  $\Delta R$  value of  $335 \pm 85$  a applicable to the Canadian Arctic Archipelago (Coulthard *et al.*, 2010), and are shown in calibrated years AD. For details of radiocarbon samples, see Table 1.

44997, 19 cm; Table 1), only barely overlapping at  $2\sigma$  (Fig. 3). The three remaining radiocarbon dates on mixed benthic foraminifera and molluscs are considered reliable within the limits of their  $2\sigma$  age ranges. The molluscan material is considered to be *in situ*, as the fine nature of the enclosing sediments does not suggest winnowing or transport into the basin.

**Dinocyst/NPP analyses**

Palynomorph samples (taken at 0.5–4 cm intervals, 001E and 001F) were processed according to protocols that allow full recovery of thin-walled dinocysts (Marret and Zonneveld,

2003). Known volumes of sediment (~3–5 cc) were wet-weighed, oven-dried (~45°C), dry-weighed, and wet-sieved at 10  $\mu\text{m}$  with distilled water. Samples were then digested in cold hydrochloric (10%) and hydrofluoric (49%) acids, and subsequently sieved at 10  $\mu\text{m}$ . Concentrations were determined by marker tablet (*Lycopodium clavatum*) addition prior to acid treatment. Dinocyst influxes (cysts  $\text{cm}^{-3} \text{a}^{-1}$ ) were calculated using age-model sedimentation rates. Residues were mounted in safranin-stained glycerine jelly, and slides were scanned systematically under high-power microscopy ( $\times 400$ ). A minimum of 300 dinocysts plus associated NPP were counted from each sample.

**Table 1.** Radiocarbon dates from core 99LSSL-001. Dating was conducted by KECK Carbon Cycle AMS Facility (University of California Irvine) and NOSAMS (Woods Hole Oceanographic Institution).

Core depth (cm)	Laboratory code	Material dated	Radiocarbon age $\pm 1\sigma$ ( <sup>14</sup> C a BP)	$\delta^{13}\text{C}$ (‰)	Age range $1\sigma^a$ (cal. a AD)	Age range $2\sigma^a$ (cal. a AD)	Median probability age (cal. a AD)
99LSSL-001E							
15–18	UCIAMS-27450	Mixed benthic foraminifera	920 $\pm$ 60	n.d.	1638–1877	1543–1950	1739
19	OS-79112	Polychaete organic tube*	1410 $\pm$ 25	–18.97	1247–1398	1148–1453	1310
36–40	UCIAMS-27451	Mixed benthic foraminifera	990 $\pm$ 150	n.d.	1498–1819	1423–1950	1663
99LSSL-001F							
19	UCIAMS-44997	Mollusc shell fragments	1100 $\pm$ 20	n.d.	1478–1633	1410–1704	1555

<sup>a</sup> Age range  $1\sigma$  probability and  $2\sigma$  probability = 1 in all cases. All radiocarbon dates have been normalized to a  $\delta^{13}\text{C}$  value of  $-25\text{‰}$  and were calibrated using CALIB 6.0 (Stuiver *et al.*, 2010) based on the marine calibration dataset Marine09 (Reimer *et al.*, 2009), with a  $\Delta R$  value of  $335 \pm 85$  a for the Canadian Arctic Archipelago (Coulthard *et al.*, 2010). \*This date was excluded from the construction of the age–depth model. n.d., no data.

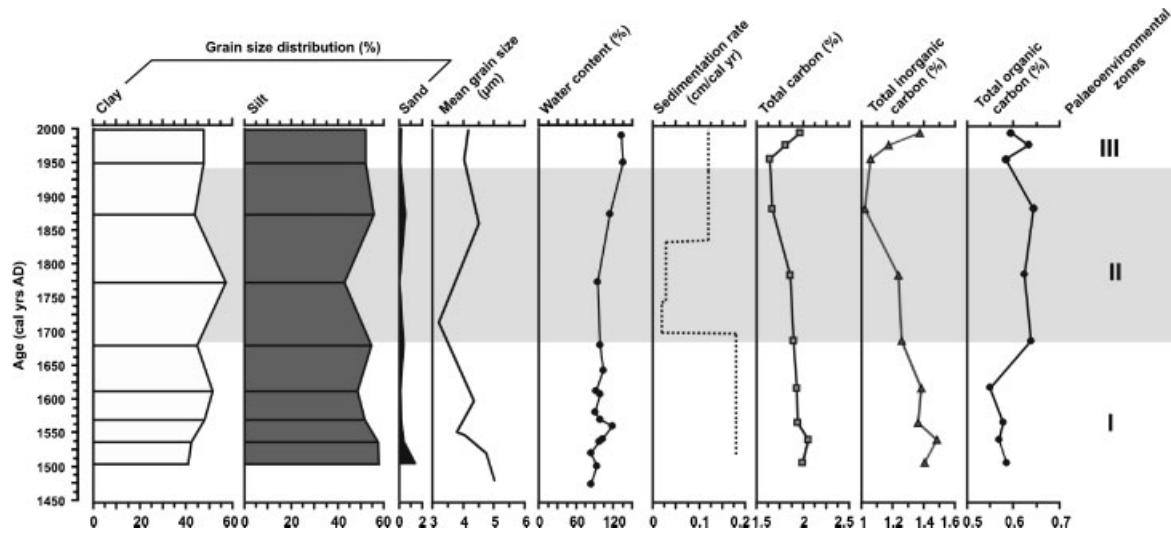


**Figure 3.** Results of sediment analyses on core 99LSSL-001, including grain size distribution and average grain size, sedimentation rate, water content (corrected for salinity), total carbon (TC) and total organic carbon (TOC).

Dinocysts were identified using Mudie (1992), Kunz-Pirrung (1998), Rochon *et al.* (1999), and Head *et al.* (2001). *Spiniferites elongatus* s.l. encompasses *Spiniferites elongatus*, *Spiniferites frigidus* and intergrade morphotypes, whereas *Islandinium cezare* s.l. groups together *Islandinium? cezare* and *Echinidinium karaense*. Within *Operculodinium centrocarpum*, we distinguished *O. centrocarpum*, *O. centrocarpum* short processes, *O. centrocarpum* var. *cezare*, and *O. centrocarpum* Arctic morphotypes. Certain dinocyst genera could not be identified to species level due to folding or obscured archaeopyle. This included *Spiniferites* spp. and *Protoperidinium* spp. which encompassed all round brown cysts that were folded or torn and could not be assigned to cyst genera. *Brigantedinium* spp. encompassed round brown cysts, including *B. simplex* and *B. cariacoense*, as well as *Brigantedinium*-type cysts in which the archaeopyle was not present or visible (*Brigantedinium* sp.). Within *Polykrikos* we distinguished Arctic morphotypes (Kunz-Pirrung, 1998) and an unknown small species, *Polykrikos* sp. A (cf. Mudie and Short, 1985). We identified *Polykrikos schwartzii* sensu Rochon *et al.* (1999) but note that this taxon may also encompass *Polykrikos kofoidii* according to Matsuoka *et al.* (2009). The ratio of predominantly autotrophic to heterotrophic dinocysts (A:H ratio) was used as a source of palaeoenvironmental information on the principal trophic mode (Mudie and Rochon, 2001). Taxa assigned to the categories of autotrophic (A) and heterotrophic (H) are listed in Fig. 4(a).

Prasinophytes and acritarchs were identified using Roncaglia (2004), Roncaglia and Kuijpers (2004), Bérard-Therriault *et al.* (1999), and Mudie *et al.* (2011). We distinguished two acritarch taxa of unknown biological affinity: acritarch P resembling Cyst P of Mudie in Scott *et al.* (1984), and a large, thin-walled leiosphere, acritarch Q. Microforaminiferal linings were classified sensu Stancliffe (1991).

### Pollen analysis

Pollen analysis included counts of all pollen grains, terrestrial plant spores, fungal spores, and colonial algae  $>10\ \mu\text{m}$ , counts of wood and charcoal particles  $>20\ \mu\text{m}$ , and fibres from samples prepared for dinocyst/NPP analyses. Pollen, terrestrial and fungal spores were identified using McAndrews *et al.* (1973) and Bassett *et al.* (1978). Charcoal particles were classified using Doubleday and Smol (2005). Wood fibres were identified where possible, using Strelis and Kennedy (1967).

## Results

### Lithology

Core 99LSSL-001 consists of 43 cm (001E) to 45 cm (001F) bioturbated, soft silty mud, with a high clay content and  $<10\%$  fine sand (Figs 2 and 3). The top 6–8 cm (ca. AD 1936–1907 AD) are red-brown (Munsell Colour 5YR 6/3), with horizontal streaks and pinworm tubes (Fig. 2), grading to soft, dark-olive mud (5Y 3/2) with small ( $<0.5\ \text{cm}$ ), round burrows. Unidentified bivalve fragments were recorded at 19 cm (ca. AD 1695). Framboidal pyrite in pollen samples  $\geq 15\ \text{cm}$  (before ca. AD 1772) suggests subsurface reducing conditions. Water content (85–136%) increases towards the core top, and grain size measurements show well-sorted mud, with peaks in the fine-silt range (Fig. 3). Textural variations downcore include poorly sorted, coarse silt and fine sand, peaking at 10 cm (ca. AD 1872), 20 cm (ca. AD 1678) and 35–40 cm (ca. AD 1536–1503; Figs 2 and 3). TOC values are relatively uniform (0.5–0.6%), whereas total inorganic carbon (TIC) is slightly elevated at the bottom and top of the record (Fig. 3). Total carbon (TC) values are high (1.6–2.1%) compared to adjacent channels (Amundsen Gulf: McLaughlin *et al.*, 2009; Dease Strait: Ledu *et al.*, 2010a), but are similar to Lancaster Sound values (Macko *et al.*, 1985).

### Smear slides

Smear slides (taken at 5 cm intervals; 001F) show angular quartz/feldspar grains in the silt/fine-sand fraction throughout the core. Abundant diatoms consist mainly of large, thin-walled and smaller *Melosira*-type centrics, with frequent small pinnate species. Echinoderm spicules are common. Several half-cells of the radiolarian *Distephanus spectabilis* were encountered at 0–8 cm (ca. AD 1907–1999), occasional resting spores of cf. *Biddulphia* being found at  $>20\ \text{cm}$  (before ca. AD 1678). No foraminifera were observed in the smear samples.

### Dinocysts and other NPP

Core 99LSSL-001 (composite of 001E and 001F) shows well-preserved dinocysts, with a total diversity of 14 species and 24 other taxa (including varieties, morphotypes, and species complexes; Figs 4a and 5; Supporting information, Fig. S1 and Table S1). Concentrations (1550 to 3990 cysts  $\text{g}^{-1}$ ) average  $\sim 2630\ \text{cysts}\ \text{g}^{-1}$ , whereas fluxes (2918 to

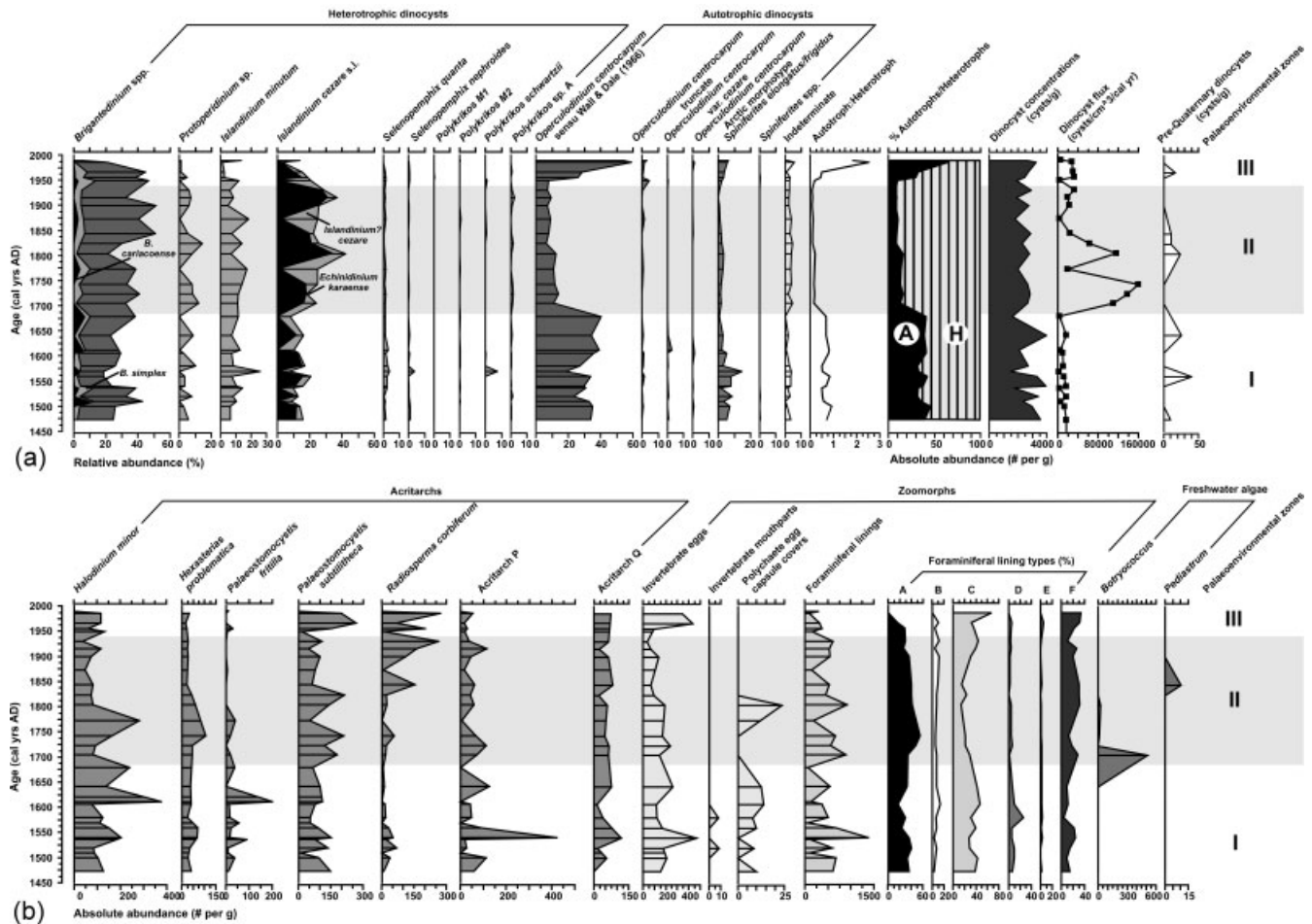


**Figure 4.** Results of organic-walled microfossil analyses on core 99LSSL-001, showing (a) dinoflagellate cyst and (b) other non-pollen palynomorphs. The taxa groupings of autotrophic and heterotrophic dinocysts shown here were used to calculate the A:H (autotrophic:heterotrophic) ratio to determine the predominant trophic mode. All plots were constructed in the C2 program (Juggins, 2007). See supporting Table S1 for a full list of taxa present and for taxonomic designations.

159 407 cysts  $\text{cm}^{-3} \text{a}^{-1}$  average 32 575 cysts  $\text{cm}^{-3} \text{a}^{-1}$ . Higher concentrations occur at core bottom and top, whereas fluxes exhibit two prominent mid-record peaks (Fig. 4a). Assemblages are dominated by five taxa, most having been reported from seasonally ice-covered regions: the heterotrophs *Brigantedinium* spp., *Islandinium? cezare*, *Echinidinium karaense*, *Islandinium minutum*, and the autotroph *Operculodinium centrocarpum*. *I. minutum* and *Brigantedinium* spp. co-dominate surface sediments in Parry Channel (Mudie and Rochon, 2001). *Brigantedinium* spp. are cysts of a cosmopolitan, heterotrophic *Protoperidinium* species complex found within a broad environmental range (Marret and Zonneveld, 2003). In Arctic Canada, *Brigantedinium* is most abundant in areas influenced by river runoff or upwelling (Mudie and Rochon, 2001; Richerol *et al.*, 2008a). *I. minutum* generally marks high latitudes where summer and winter sea surface temperatures are 7°C and 0°C, respectively (Rochon *et al.*, 1999; Head *et al.*, 2001). The common polar taxa *I.? cezare* and *E. karaense* may be particularly sensitive to extensive sea-ice (Matthiessen *et al.*, 2005), although rare *I.? cezare* have been found in temperate Atlantic marsh sediments (Pospelova *et al.*, 2004, 2005). Arctic morphotypes (M1, M2) of the phagotrophic genus *Polykrikos*, considered polar indicators (Kunz-Pirring, 1998), are sparse throughout core 99LSSL-001. The autotroph *O. centrocarpum* is rare within the north-central CAA, abundances increasing in areas characterized by longer open-water seasons (Mackenzie Shelf, western Amundsen Gulf; Mudie and Rochon, 2001; Richerol *et al.*, 2008a).

Abundant and diverse NPP characterize core 99LSSL-001 (Figs 4b and 5; supporting Table S1), in contrast to Dease Strait (*Halodinium* and microforaminiferal linings only, Ledu *et al.*, 2010a). Coronation Gulf assemblages are composed of acritarchs, zoomorphs (invertebrate mouthparts and eggs, microforaminiferal linings, tintinnid loricae), colonial freshwater algae (*Botryococcus*, *Pediastrum*) and rare desmids (*Cosmarium* type). Most prominent are acritarchs *Halodinium minor* (max. ~380 individuals  $\text{g}^{-1}$ ), *Radiosperma corbiferum*, and *Palaeostomocystis subtilithea* (max. ~270 individuals  $\text{g}^{-1}$ ), and microforaminiferal linings (max. ~680 linings  $\text{g}^{-1}$ ). *H. minor*, associated with cool brackish/fresh surface waters, has been found in a variety of sub-Arctic to Arctic environments (Mudie and Harland, 1996; Roncaglia and Kuijpers, 2004). *P. subtilithea*, possibly the lorica of an *Acanthostomella* spirotrich (cf. Bérard-Therriault *et al.*, 1999), was described from Greenlandic waters (Roncaglia, 2004), having previously been reported for Baffin Island fjords (as *Pterosperma*; Mudie, 1992). It appears to be associated with low-salinity stratified waters. Microforaminiferal linings are one of the most common NPP and show five distinct forms (Figs 4b and 5): biserial (forms A, B), trochospiral (chambers discrete: C; chambers overlap: D), planispiral (chambers discrete: E), and miscellaneous other types (F) (Stancliffe, 1991). Other NPP (e.g. *Neorhabdocoela*-type polychaete egg capsule covers) show minor frequencies and/or are present at sporadic intervals (Fig. 4b). Tintinnids resembling types E and P of Reid and John (1978) are common in surface sediment (<8 cm; after ca. AD 1907).

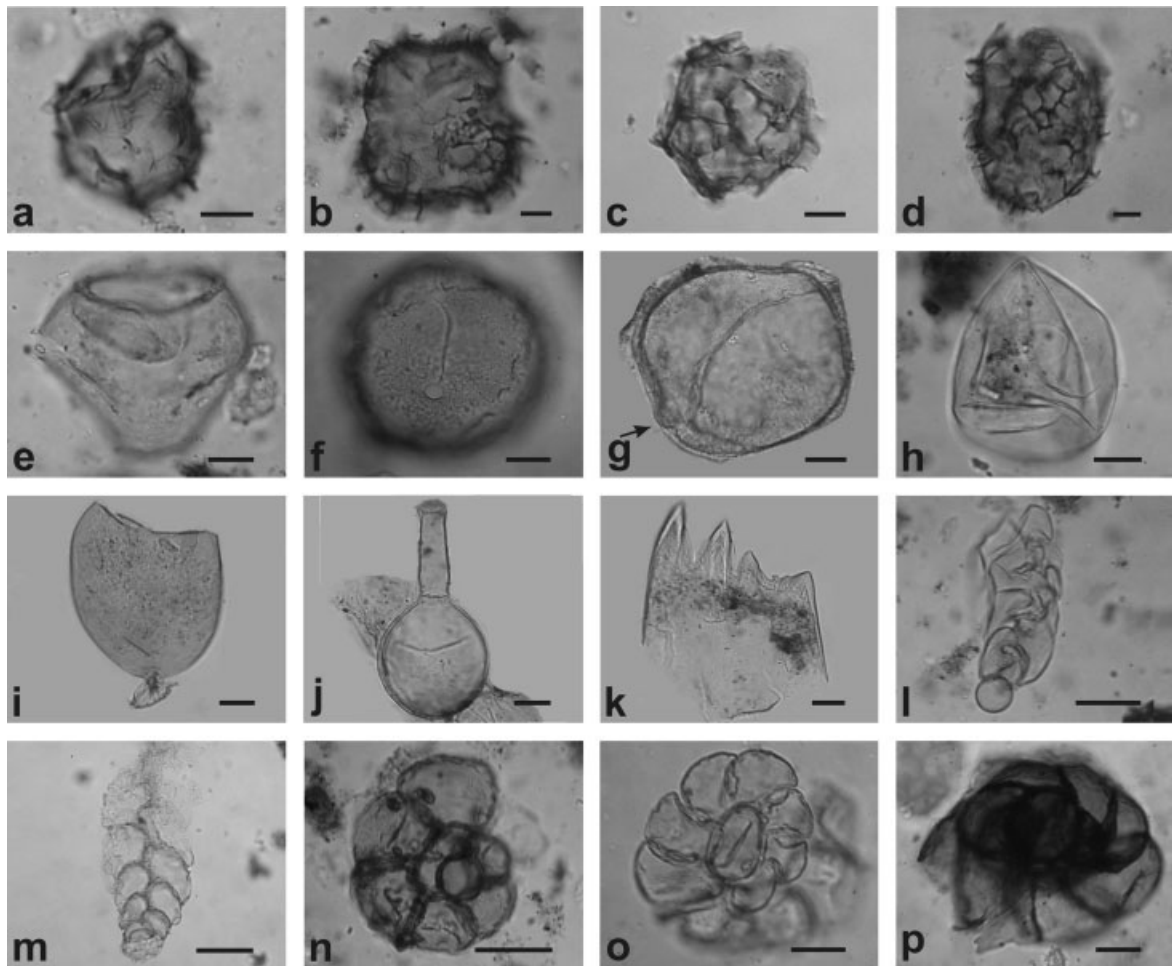


**Figure 5.** Photos of selected organic microfossils from Coronation Gulf. (a–d) Dinoflagellate cysts; (e–p) non-pollen palynomorphs. Scale bars denote 10  $\mu\text{m}$  (a–d) or 20  $\mu\text{m}$  (e–p); sample code, core depth and England finder coordinates, where available, are given in parentheses. (a, b) *Polykrikos* Arctic morphotypes (a) M1 and (b) M2 *sensu* Kunz-Pirrung 1998 (a: XII1/1; F 22–23 cm; G31/3; b: XII2/4; F 25–26 cm; G56/3). (c) *Polykrikos* sp. A (XII5/1; F 34–35 cm; Y67/1). (d) *Polykrikos schwartzii* (XIV7/1; F11–12 cm; T62/2). (e) *Palaeostomocystis subtilithea* in lateral view (XII6/3; F 37–38 cm; R34/1). (f, g) Acritarch P in (f) apical view (II4/14; E 14–16 cm; Y27/1), with the protracted pylome indicated by arrows in (g) (E 12–13 cm). (h) Acritarch Q (XII2/3; F 25–26 cm; N49/4). (i) Polychaete egg capsule cover (F 44–45 cm). (j) Tintinnid lorica (F 7–8 cm). (k) Invertebrate mouthpart (F 34–35 cm). (l–p) Microfaminiferal lining types A (XIV6/3; F 8–9 cm; H50/2), B (XII4/3; F 31–32 cm; G67/2), C (XIV6/3; F 8–9 cm; S51/2), D (XIV7/1; F 11–12 cm; L65/3) and E (XIV10/4; F 16–17 cm; U36/2). Foraminiferal lining type F is not pictured here because it groups miscellaneous lining forms.

### Pollen, spores and charcoal

Total pollen and spore concentrations (composite 001E and 001F) are low (average  $\sim 1000 \text{ g}^{-1}$  dry weight), but show a twofold increase downcore (Fig. 6). Low concentrations are typical of Arctic marine environments (Mudie, 1982); however, Coronation Gulf pollen concentrations are higher than those reported in Dease Strait (mean  $\sim 100 \text{ grains cm}^{-3}$ ; Ledu *et al.*, 2010a). Assemblages are dominated by *Pinus*, particularly the small grains of *P. banksiana*, and variable amounts of *P. resinosa* and *P. strobus* (grouped as *Pinus* spp.). *Picea mariana* and *P. glauca* are also abundant, whereas *Abies* is rare. Other Arctic arboreal pollen types (e.g. *Juniperus*, *Populus*, *Betula*, *Salix*) occur in minor amounts. Herb and moss pollen comprise 10–20% of the total pollen and spores. Herb pollen are dominated by wind-transported Arctic species (Poaceae, Cyperaceae), with a low diversity and variable amounts of *Saxifraga*, *Potentilla* and other Rosaceae, and including *Artemisia*, Chenopodiaceae and *Oxyria* (Fig. 6). Small amounts of insect-pollinated ericaceous pollen are occasionally present (included in Fig. 6 with Indeterminate). Pteridophyte spores are rare, but include *Polypodium*- and *Pteridium*-type spores. Bryophyte spores encompass several *Sphagnum* spp. and unknown *Bryales*; the latter are only common at the core top,

whereas *Sphagnum* generally increases downcore, peaking at 15 cm (ca. AD 1772).

Micro-charcoal concentrations are low ( $< 500 \text{ g}^{-1}$ ), but shows large peaks at 30 cm (ca. AD 1569) and 15 cm (ca. AD 1772), corresponding to maxima in 'lacy' charcoal fibres and non-carbonized wood fibres/vessels (Fig. 6). Other charcoal particles – small rods or spheres with angular margins – resemble the environmental combustion particles of Doubleday and Smol (2005, plates 8 and 10). Microfibres include occasional strands of natural and/or synthetic material: flax, hemp and cotton ( $> 20$  cm; before ca. AD 1678), and silk or synthetic fabric ( $< 16$  cm; post ca. AD 1752).

### Palaeoenvironmental zones

Core 99LSSL-001 was subdivided into three time intervals (zones I–III), based on major changes in different palaeoenvironmental parameters derived from sediment characteristics, dinocyst, NPP, pollen and charcoal data (Figs 2–4 and 6). Sedimentologically, the core shows subtle variations, including reducing conditions  $> 7$  cm (before AD 1923), and increased sand, scattered granules, and larger burrows  $> 20$  cm (prior to ca. AD 1678). Dinocysts show the most prominent changes of all microfossils studied; their environmental preferences (sea

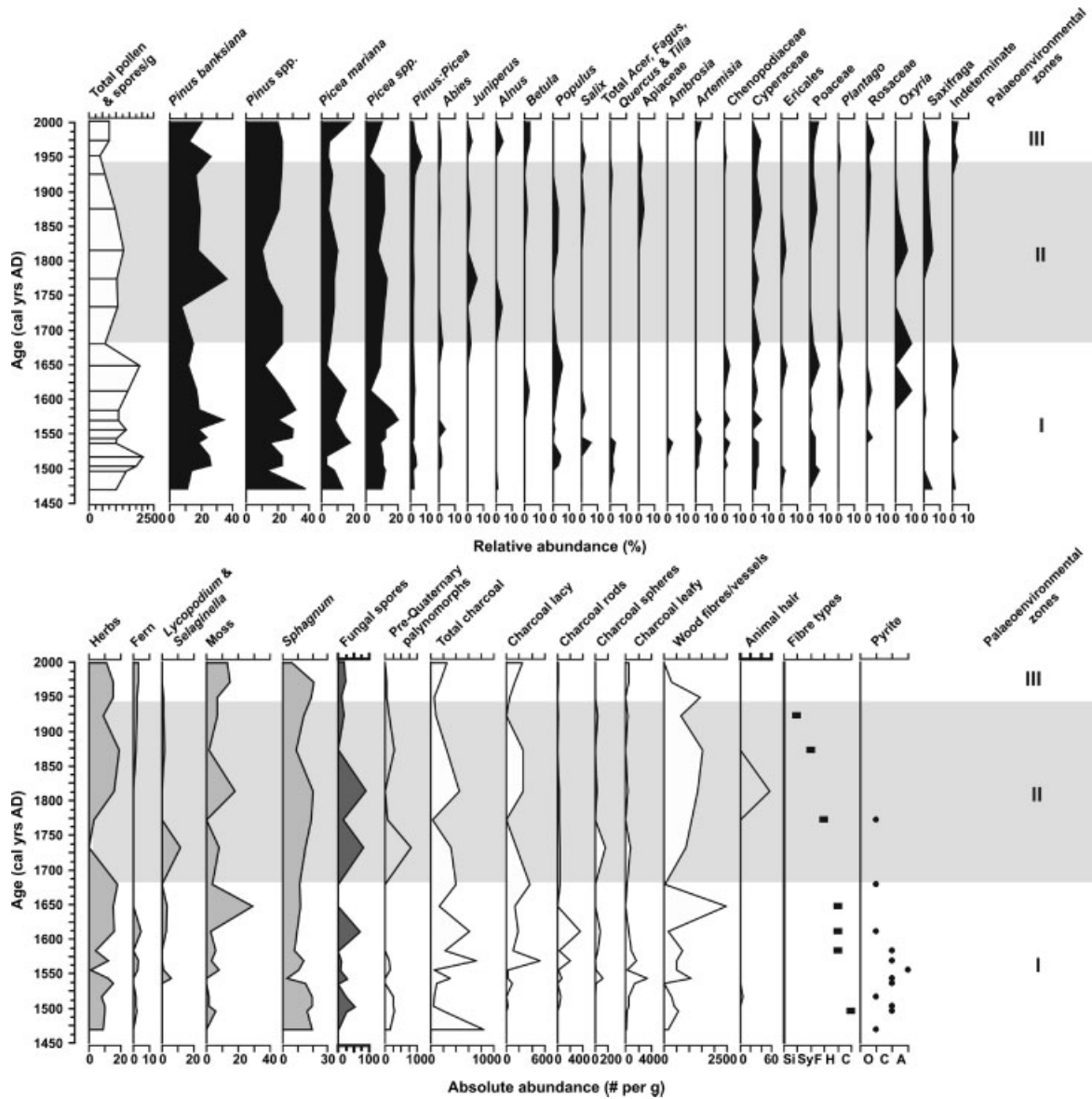


**Figure 6.** Results of pollen and spore analyses, as well as charcoal and wood fragment analyses on core 99LSSL-001, drawn in C2 (Juggins, 2007). Abbreviations: O, occasional; C, common; A, abundant. Fibre types: C, cotton; F, flax; Si, silk; Sy, synthetic.

surface temperature, salinity, sea-ice) being relatively well defined (e.g. Rochon *et al.*, 1999; Marret and Zonneveld, 2003). In contrast, NPP are largely enigmatic (e.g. Roncaglia, 2004; Mudie *et al.*, 2011), their link to Arctic (palaeo)environmental conditions being only qualitatively understood.

*Zone I (45–20 cm; ca. AD 1470–1680)*

**Characteristics.** Mud with coarse silt and fine sand, and decreasing TOC characterize this zone (Figs 2 and 3). Most notable are high relative abundances of the gonyaulacoid *O. centrocarpum* (including several morphotypes) along with lesser (but elevated compared to other zones) abundances of *S. elongatus* s.l. These are accompanied by protoperidinoids (*Brigantidium* spp., *I. minutum*, *I. cesare* s.l.). Relatively high A:H ratios (0.5–0.9; Fig. 4a) reflect the dominance of the mostly phototrophic gonyaulacoids. Concentrations of the acritarchs P and Q, invertebrate eggs, polychaete egg capsules, and microforaminiferal linings (types A and C, with lesser type D) are elevated (Fig. 4b). Pollen concentrations are high, assemblages predominantly consisting of coniferous (~50%) and deciduous (5%) forest tree pollen (*Acer*, *Fagus*, *Quercus*, *Tilia*; Fig. 6).

**Interpretation.** Zone I marks a climatic amelioration with an extended open-water season. Most dinocysts prevalent in Zone I co-dominate modern Parry Channel assemblages (Mudie and Rochon, 2001). However, the high *O. centrocarpum* abundance (19–40%) contrasts with present-day CAA assemblages (~7%; Mudie and Rochon, 2001), but is similar to proportions seen in adjacent areas (Beaufort Shelf; Mudie and Rochon, 2001; Richerol *et al.*, 2008a) and nutrient-enriched North Atlantic waters (Marret and Zonneveld, 2003). Similarly, *S. elongatus* s.l. is near-absent from the modern CAA, but occurs in Baffin Bay (Mudie and Rochon, 2001), the Beaufort Shelf and Amundsen Gulf (Richerol *et al.*, 2008a), and along Atlantic or Pacific water inflow (Kunz-Pirrung, 1989; Marret and Zonneveld, 2003; Matthiessen *et al.*, 2005).

Zone I A:H ratios are consequently closer to central Baffin Bay and Beaufort Shelf values (Mudie and Rochon, 2001; Richerol *et al.*, 2008a). Autotrophic dinocysts are directly governed by abiotic factors (light availability, nutrients) rather than by prey availability (Matthiessen *et al.*, 2005). High A:H ratios thus suggest decreased ice cover and more open water (likely more than the 2–3 months per year recorded in the 20th century by Pharand, 1984), greater light penetration (Wang *et al.*, 2005; Richerol *et al.*, 2008b), and possible nutrient

enrichment from increased river inflow. Relatively abundant zoomorphic NPP also imply high planktonic and benthic secondary-level production. The relatively elevated total coniferous tree pollen and occasional influxes of temperate tree pollen indicate long-distance transport by southerly winds (Bourgeois *et al.*, 1985; Bourgeois, 2000) in addition to transport from rivers with headwaters in, and south of, the Great Slave Region. Small *Salix* peaks also imply an expansion of local shrub tundra vegetation, consistent with a wetter, warmer climatic period. Elevated fine sand/coarse silt percentages and TIC (Fig. 3) may indicate increased ice-rafted debris (IRD) deposition from carbonate bedrock sources due to local sea-ice mobility and melting and/or increased runoff. The pre-Quaternary palynomorphs, predominantly bisaccate pollen and Palaeozoic spores, indicate redeposition from Palaeozoic terrigenous sediment sources rather than local Proterozoic bedrock. The relatively high rate of inorganic sediment deposition may explain the comparatively low dinocyst fluxes in this biologically productive zone.

#### Zone II (20–6 cm; ca. AD 1680–1940)

**Characteristics.** Zone II displays a decrease in coarse silt/fine sand and TIC, and a rise in clay (Fig. 3). *O. centrocarpum* and *S. elongatus* s.l. abundances decline, whereas *I. cezare* s.l. increases. A:H ratios (0.09–0.21) are much lower than in Zone I. *I. minutum* concentrations are unchanged, while *Brigantedinium* spp. proportions are elevated (Fig. 4a). *H. minor* and *P. fritilla* concentrations are reduced, whereas *R. corbiferum* abundances rise upzone. Abrupt peaks of the fresh/brackish water algae *Botryococcus* and *Pediastrum* occur at the zone base and top, respectively. Microforaminiferal lining concentrations, especially type A, increase (Fig. 4b). Pollen and spore abundances decrease; however, *Juniperus*, Ericaceae and the common Arctic herbs *Oxyria* and *Saxifraga* rise (Fig. 6). Fungal spores and pre-Quaternary pollen/spores peak, along with greater abundances of charcoal particles and wood fibres (Fig. 6). Unidentified animal hair peaks at ~15 cm (ca. AD 1725).

**Interpretation.** This zone marks increased seasonal sea-ice and generally colder, more polar conditions, as indicated by a decline in autotrophic dinocysts (*O. centrocarpum*, *S. elongatus* s.l.) and lower A:H ratios. Large increases in heterotrophic dinocyst fluxes may reflect enhanced under-ice algae production (i.e. potential food sources), an important contributor to annual net productivity (~40% in Amundsen Gulf; Elizabeth Henderson, pers. comm., 2010). However, the high dinocyst fluxes may also reflect the lowered sedimentation rates within this zone (Fig. 3). Increases in *I. cezare* s.l. (>15%) are also important because in relatively high percentages they are generally considered particularly sensitive indicators of pervasive sea-ice (Head *et al.*, 2001; Matthiessen *et al.*, 2005). Maximum *I. cezare* abundances in Zone II are comparable to those reported for the Mackenzie Shelf (Richerol *et al.*, 2008a), but contrast with Parry Channel (~9%; Mudie and Rochon, 2001).

The increases in freshwater–brackish indicators (Mudie, 1992; Matthiessen *et al.*, 2000; Mudie *et al.*, 2011) may suggest episodes of lowered salinity during Zone II. *R. corbiferum*, indicative of fluvial input, has been described from temperate to polar environments (e.g. Matthiessen *et al.*, 2000). Spikes of the freshwater–brackish colonial algae (*Botryococcus*, *Pediastrum*) may indicate freshwater discharge into Coronation Gulf, either from increased fluvial input (Matthiessen *et al.*, 2000) or flooding onto sea-ice (cf. Mudie, 1992; Pfirman *et al.*, 1989). Lowered total pollen concentrations, and relative increases in *P. banksiana*, juniper, heaths and tundra herbs, suggest colder

climate. Reduced wood charcoal may indicate a decrease in forest fire frequency. Increases in fungal spores, including *Glomus*, may indicate greater influx of eroded sediment (Mudie *et al.*, 2011). Although elevated percentages of fine sand/coarse silt characterize the start and end of Zone II (Fig. 3), possibly indicating increased fluvial input and sea-ice IRD, these bracket an interval of increased clay and reworked (pre-Quaternary) dinocyst deposition. This fine-grained IRD-poor interval within the central part of Zone II may indicate a longer interval of landfast (immobile) sea-ice limiting IRD deposition (cf. Dowdeswell *et al.*, 2000; Ó Cofaigh and Dowdeswell, 2001) or a change in sea-ice trajectory. Collectively, these data imply a period of climatic deterioration marked by greater sea-ice and lower temperatures.

#### Zone III (6–0 cm; ca. AD 1940–1999)

**Characteristics.** The red-brown colour, abundant streaks and pinworm burrows, and elevated TIC values distinguish Zone III (Figs 2 and 3). Despite bioturbation, palynomorphs show clear trends: *O. centrocarpum* increases markedly and *S. elongatus* s.l. abundance rises, whereas *I. cezare* s.l., *Brigantedinium* spp., and *I. minutum* decrease (Fig. 4a). Dinocyst assemblages are similar to Zone I, but relative *O. centrocarpum* abundances are higher. *P. subtilitheca* and invertebrate egg concentrations peak, whereas *P. fritilla* is rare (Fig. 4b). Reduced microforaminiferal linings show marked declines in types A and B, while Type C dominates; type E linings appear for the first time. Pollen concentrations increase relative to the minimum at the top of Zone II (Fig. 6). Industrial fly-ash occurs at the zone top (0–2 cm). *Sordaria* fungal spores, indicative of animal herding (Mudie *et al.*, 2011) also appear (Fig. 6). *Betula* and *Alnus* shrub pollen increase and adventive herbs (*Plantago*, *Chenopodium*, *Artemisia*) are more common, while *Pinus:Picea* ratios peak.

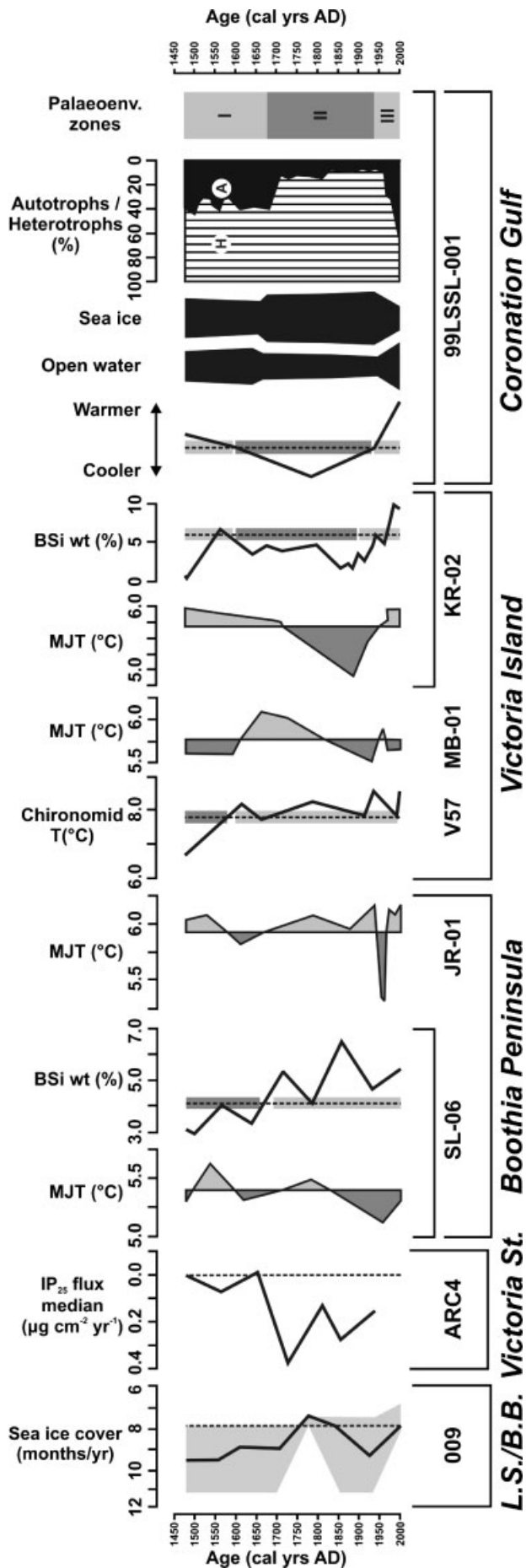
**Interpretation.** Zone III records a return to ameliorated climatic conditions, resulting in a shorter sea-ice season. While generally similar to Zone I, Zone III exhibits a more prominent *O. centrocarpum* component, higher A:H ratios and slightly greater dinocyst influxes. Cold-water taxa, particularly Arctic endemics (*I. cezare* s.l.), are notably reduced. A:H ratios (0.2–2.5) are elevated compared to Parry Channel (0.1) and the Beaufort Shelf (0.84; Mudie and Rochon, 2001), higher values being encountered in the North Water (1.27; Mudie and Rochon, 2001) and Cape Bathurst polynyas (>5; Richerol *et al.*, 2008a).

The relatively high A:H ratios suggest an extended open-water season since ca. AD 1940, with the rise in invertebrate eggs indicating increased zooplankton productivity. Zone III pollen assemblages do not imply major climatic variations, but the persistent presence of small *Betula* and reappearance of *Alnus* pollen may indicate increased low Arctic tundra vegetation relative to spruce taiga woodland. High *Pinus:Picea* ratios ca. AD 1940–1970 suggest a return of stronger southerly airflow. Elevated herb pollen concentrations may mark a time of increased forest clearance and human settlement in Kugluktuk after 1916 AD, as previously suggested by increased *Urtica* (nettle) pollen in Coppermine River delta peat (Nichols, 1975).

## Discussion

### The AD 1470–1680 interval (Zone I)

The prominence of autotrophic dinocysts and reduced sea-ice indicator proportions suggest relatively ameliorated conditions with an extended open-water season in Coronation Gulf ca. AD 1470–1680 (Fig. 7). As our record commences at ca. AD 1470,



the onset of this amelioration could not be determined. Due to a lack of regional marine data, the spatial extent of this warm period is also unknown. The closest comparable late Holocene marine studies are currently from Amundsen Gulf (~560 km northwestward; Schell *et al.*, 2008), Mackenzie Trough (~900 km northwestward; Richerol *et al.*, 2008b), and Victoria Strait (~500 km eastward; Belt *et al.*, 2010). Dease Strait cores (~250 km distant) unfortunately lack sediments younger than ca. AD 1150 (Belt *et al.*, 2010; Ledu *et al.*, 2010b). One Mackenzie Trough boxcore extends into Zone I, but its near-barren dinocyst assemblages do not show warmer conditions during ca. AD 1420–1550 (Richerol *et al.*, 2008b). This discrepancy may be attributed to temporal and spatial lags between Mackenzie Trough and Coronation Gulf, but could also be due to different chronological protocols. Specifically, Richerol *et al.* (2008b) do not report the conventional <sup>14</sup>C age or ΔR used for calibration, so that the correlative potential of the two records is impossible to assess. Farther east in Victoria Strait, however, the sea-ice diatom biomarker IP<sub>25</sub> infers reduced spring sea-ice AD 1400–1600 (Belt *et al.* 2010; Fig. 7), in agreement with our data. During approximately the same interval, dinocyst-based transfer functions also imply reduced sea-ice in Barrow Strait, but increased sea-ice in Lancaster Sound/Baffin Bay (Ledu *et al.*, 2010a,b), potentially indicating the influence of the Arctic Oscillation.

Terrestrial archives from Victoria Island and the mainland allow for regional comparison of Zone I conditions (Figs 1 and 7). Our pollen data show good agreement with onshore pollen assemblages from two Coppermine River peat sections (Nichols, 1975). However, some terrestrial archives show disparity with our data during this time, as well as between subregions (e.g. MacDonald *et al.*, 2009; Peros and Gajewski, 2008, 2009; Porinchu *et al.*, 2009; Fig. 7). Such incongruities may reflect differing chronological approaches, as well as the environmental sensitivities of, and calculation techniques used for, different proxies. Nonetheless, these apparent discrepancies may also reflect a genuine heterogeneity in environmental response to late Holocene climate change. Regional records broadly correlative with our amelioration include pollen-based reconstructions on western Boothia Peninsula (warming ca. AD 1000–1500; Zabenskie and Gajewski, 2007; Peros and Gajewski, 2009), and pollen and chironomid assemblages from northern Victoria Island (warming ca. AD 300–1700; Peros and Gajewski, 2008, 2009; Fortin and Gajewski, 2010). Conversely, other Boothia records generally suggest deteriorating climate during 1200–1400 AD (LeBlanc *et al.*, 2004; core SL06, Zabenskie and Gajewski, 2007; MacDonald *et al.*, 2009; Paul *et al.*, 2010).

Our marine pollen records are expectedly biased by wind-blown tree pollen (Mudie, 1982) derived from the nearest

**Figure 7.** Comparison of palaeoenvironmental reconstructions from core 99LSSL-001 and other, regional records (Fig. 1a). Pollen-based quantitative reconstructions of mean July temperature (MJT) for lakes MB01 and SL06 by Peros and Gajewski (2009), who also recalculated pollen records of lakes KR02 (Peros and Gajewski 2008) and JR01 (Zabenskie and Gajewski 2007). Records of biogenic silica (BSi) tracing siliceous algal productivity is shown from lakes KR02 (Peros and Gajewski, 2008) and SL06 (Peros and Gajewski, 2009). Chironomid-derived temperature reconstructions from Porinchu *et al.* (2009). Above-average warmer and cooler temperatures are indicated by light and dark grey bars respectively, for the aforementioned studies. Sea-ice diatom pigment (IP<sub>25</sub>) data are from Victoria Strait (core ARC4; Belt *et al.*, 2010). Dinocyst-based reconstructions of sea-ice cover (with standard error in grey) are from a boxcore at the entrance of Lancaster Sound (L.S.) in Baffin Bay (B.B.; core 009; Ledu *et al.*, 2008, 2010a, b). All data from other studies were reported in calibrated years AD.

forests: spruce–poplar scrub (today 15 km inland, Coppermine River valley) and spruce–pine forest at the boreal forest limit (today ~150 km south of Coronation Gulf), or even farther away. The exclusive presence of some deciduous forest tree pollen (*Acer*, *Fagus*, *Quercus*, *Tilia*), and the consistent presence of the relatively large pollen of *Abies* are good indicators of transport by southerly winds and/or river water during AD 1470–1680. Peaks in *Pinus*, *Alnus* and *Betula* pollen in CAA ice cores may indicate stronger southerly (i.e. warmer) winds during spring (Bourgeois, 2000).

The amelioration in Zone I may correspond to the Mediaeval Warm Period (MWP) or, alternatively, the MWP–Little Ice Age (LIA) transition. Although generally considered to have ended by ca. AD 1400, the spatial (global) and temporal extents of the MWP have been debated (e.g. Maasch *et al.*, 2005; Osborn and Briffa, 2006; Mann *et al.*, 2009). Several palaeoenvironmental studies have identified the MWP within the CAA (e.g. Koerner, 1977; Mudie *et al.*, 2005; Podrilske and Gajewski, 2007), including southern Boothia Peninsula (MWP ca. 1150–600 cal. a BP; ≈AD 800–1350; LeBlanc *et al.*, 2004; ca. 900–750 cal. a BP; ≈AD 1050–1200; Zabenskie and Gajewski, 2007) and northern Victoria Island (ca. 1500–800 cal. a BP; ≈AD 500–1200; Fortin and Gajewski, 2010). Although these terrestrial studies suggest MWP termination prior to Zone I, the possibility of a lag between marine and terrestrial systems exists. However, given the current lack of regional marine studies, any link to the MWP must remain speculative. Further research should clarify the regional and temporal extent of the amelioration, and will determine how representative and/or widespread Zone I conditions are beyond Coronation Gulf.

### The AD 1680–1940 interval (Zone II)

Both our marine and terrigenous palynological data suggest cool conditions with increased sea-ice and a shorter open-water season ca. AD 1680–1940 (Fig. 7), evident in a rise of sea-ice indicators, and decreasing autotrophic dinocysts. This may mark the onset of the LIA in Coronation Gulf, also identified in Mackenzie Trough dinocyst assemblages (ca. AD 1550–1850; Richerol *et al.*, 2008b), Victoria Strait IP<sub>25</sub> values (ca. AD 1500–1900; Belt *et al.*, 2010), and Amundsen Gulf foraminifera (<100 cal. a BP; ≈AD 1850; Schell *et al.*, 2008). This contrasts with Lancaster Sound/Baffin Bay, where dinocyst transfer functions suggest warming ca. AD 1650–1900 (Ledu *et al.*, 2008).

Regional terrestrial records vary in the temporal extent of a recent cooling event correlative to Zone II (Fig. 7). Kugluktuk pollen assemblages (Nichols, 1975) show colder, drier summers and declining exotic pollen ca. 500–230 <sup>14</sup>C a BP (≈1425–1660 AD), with an increase in Ericales also seen later in Zone II in Coronation Gulf (ca. AD 1813). Mainland lakes show LIA conditions marked by lowered surface-water temperatures and biological productivity ca. AD 1300/1390–1850 (treeline; MacDonald *et al.*, 2009; east of Bathurst Inlet; Paul *et al.*, 2010). In contrast, other mainland sites suggest that cooling commenced AD 1200–1400 (LeBlanc *et al.*, 2004; Zabenskie and Gajewski 2007; MacDonald *et al.*, 2009; Paul *et al.*, 2010). Victoria Island records are more cryptic. LIA onset is suggested ca. AD 1100–1250 in the south, with an anomalous warm event ca. AD 1600 (MB01; Peros and Gajewski, 2009; Porinchi *et al.*, 2009) before cooling. Northern Victoria Island cores (KR02; Peros and Gajewski, 2009; WB02; Fortin and Gajewski, 2010), however, show a marked delay in cooling, commencing ca. AD 1700 (Fig. 7).

Within the CAA, the LIA has been more widely recognized than the MWP. Ice caps on Devon, Meighen, and Ellesmere islands (Fig. 1a) show colder conditions ca. 400–100 a BP, when sea-ice shelves may have also reached their Holocene

limit (Koerner and Paterson, 1974; Koerner, 1977; Koerner and Fisher, 1990; Bradley, 1990). Low sea-salt deposition on the Penny Ice Cap (Baffin Island; Fig. 1a) suggests severe sea-ice AD 1400–1900 in Baffin Bay (Grumet *et al.*, 2001). Vegetation trimlines attributed to dropping snowlines during the LIA have been mapped throughout the CAA (Wolken *et al.*, 2005), and colder LIA summers characterized by increased rainfall have been identified in lacustrine records, suggesting the entry of widespread synoptic-scale storm systems into the central archipelago (Lamoureux *et al.*, 2001).

Although the onset and termination of cooler conditions shows regional heterogeneity (Gajewski and Atkinson, 2003), a pan-Arctic cooling trend has been recognized in the recent past (Overpeck *et al.*, 1997), the CAA showing coldest Holocene conditions ca. AD 1550–1900 (Bradley, 1990). Harsh conditions are also apparent from early instrumental air temperature records compiled by the Hudson Bay Company (AD 1751–1870; Houston *et al.*, 2003), and British Navy expeditions into the Northwest Passage (1800s; Przybylak and Vizi, 2005). The palaeoenvironmental data from Coronation Gulf all suggest a cooler, sea-ice characterized interval during the 17th to early 20th century, similar to LIA cooling in northern Baffin Bay (sea-ice diatom peaks at AD 1750 and 1550; Knudsen *et al.*, 2008), and in accord with GISP and North Icelandic shelf records ca. AD 1700–1900 (Knudsen *et al.*, 2004). This stands in contrast to West Greenland (Disko Bugt) and areas on the Labrador and Nova Scotia slopes, where only minimal oceanographic changes occurred during the LIA (Keigwin and Pickart, 1999; Keigwin *et al.*, 2003; Seidenkrantz *et al.*, 2008).

### The AD 1940–2000 interval (Zone III)

Our data indicate substantial sea-ice decrease and an extended open-water season in Coronation Gulf since ca. AD 1940, in accordance with historical ship-based observations (Headland, 2010). This warming, evident in a prominent shift from a heterotroph- to autotroph-dominated dinocyst community (Fig. 7), suggests a greater amelioration than that proposed during Zone I (ca. AD 1470–1680). This implies longer ice-free conditions and higher nutrient availability during the 20th century. Such dominance of autotrophic dinocysts has not been described previously from the CAA, where heterotrophs dominate modern sediments without exception (Mudie and Rochon, 2001). Within the context of the CAA channels, the high relative abundance of autotrophs in Coronation Gulf is therefore extraordinary, and parallels the exceptional and non-analogous diversification of lacustrine diatoms since the late 19th century across the archipelago (Smol *et al.*, 2005).

Zone III conditions are in keeping with sea-ice reduction during the past ~100 years in Amundsen Gulf (Schell *et al.*, 2008) and since ca. AD 1850 in Mackenzie Trough (Richerol *et al.*, 2008b), but contradict Barrow Strait and Lancaster Sound records (Ledu *et al.*, 2010b). The majority of regional terrestrial records show 20th-century warming (Fig. 7), including Kugluktuk pollen assemblages (late 19th to early 20th century; Nichols, 1975), as well as lake sediments at the treeline (Rüthland and Smol, 2005; MacDonald *et al.*, 2009; Paul *et al.*, 2010), on Boothia Peninsula (LeBlanc *et al.*, 2004; Peros and Gajewski, 2009), and Victoria Island (Porinchi *et al.*, 2009; Podrilske and Gajewski, 2007; Fortin and Gajewski, 2010). Recent warming has also been reported for the broader CAA from lacustrine sequences (e.g. Smol *et al.*, 2005) and ice cores (Koerner, 1977; Koerner and Fisher, 1990), the latter possibly associated with strong southerly winds during spring (Bourgeois, 2000).

In the last few decades, Arctic spring and summer temperatures have risen and sea-ice extent and thickness have

decreased (e.g. Turner *et al.*, 2007). Since ca. AD 1925, CAA summer temperatures have been, overall, exceptionally high compared to most of the Holocene (Bradley, 1990). This warming is forecast to continue, with sea-ice effectively lost by AD 2040–2100 (Solomon *et al.*, 2007). Our data show that this prominent 20th-century warming is recorded in Coronation Gulf, and should be evident in marine sediments throughout the southwestern CAA. In contrast, dinocyst records from Lancaster Sound/Baffin Bay show relatively small changes in summer sea surface temperatures and sea-ice since ca. AD 1420 (Ledu *et al.*, 2008). This discrepancy may be attributed to decadal-scale Arctic Oscillation shifts (Turner *et al.*, 2007). However, differences in sedimentation rates ( $0.12 \text{ cm a}^{-1}$  in Coronation Gulf vs.  $0.02\text{--}0.06 \text{ cm a}^{-1}$  in Lancaster Sound/Baffin Bay; Ledu *et al.*, 2008, 2010b) and sample intervals (24–40 a in Coronation Gulf vs. ca. 80 a in Lancaster Sound/Baffin Bay) may also account for some of the apparent interregional differences.

### Late Holocene environmental change in core 99LSSL-001

Our study indicates several prominent late Holocene environmental shifts in Coronation Gulf. These changes consist of a succession from relatively warm, seasonally ice-free conditions ca. AD 1470–1680 (Zone I) to a colder period characterized by more extensive sea-ice ca. AD 1680–1940 (Zone II), and finally 20th-century warming with reduced sea-ice since ca. AD 1940 (Zone III). These shifts appear to correspond to regional climatic trends observed on the neighbouring mainland and Victoria Island, as documented from peat section and lacustrine sediments, and with palaeoceanographic records from Amundsen Gulf and Mackenzie Trough. While marine and terrestrial environments within the CAA are intrinsically linked (Mudie and Short, 1985; England, 1987), environmental changes within one environment need not precisely reflect the shifts in the other, allowing for potential lags between and within the two realms (e.g., Devon Island; Koerner, 1977; vs. Barrow Strait; Pieńkowski *et al.*, 2011).

Nonetheless, the most recent environmental intervals (zones II, III) observed in core 99LSSL-001 correlate well with many other Arctic marine and terrestrial records. Zone I, in contrast, shows pronounced regional discrepancies. Whereas LIA cooling commences AD 1200–1400 in the central CAA and on the mainland (LeBlanc *et al.*, 2004; Zabenskie and Gajewski, 2007; MacDonald *et al.*, 2009; Paul *et al.*, 2010), cooling is delayed (ca. AD 1600–1700) on northern/north-western Victoria Island (Peros and Gajewski, 2009; Fortin and Gajewski, 2010). Southern Victoria Island records suggest an intermediate climate history, with some evidence for early (ca. AD 1100–1250) cooling, and subsequent warming, before full LIA is achieved (AD 1800; Peros and Gajewski, 2009; Porinchu *et al.*, 2009).

The use of disparate proxy records, dating methodologies, and interpretive protocols may account for the inter-record discrepancies seen during Zone I. However, given the apparent regional pattern and the good general correlation between our marine record and most regional terrestrial records, this temporal and spatial variability may indeed be real. Nonetheless, apparent differences between our record and other marine archives from Amundsen Gulf (Schell *et al.*, 2008b), Mackenzie Trough (Richerol *et al.*, 2008b), Victoria Strait (Belt *et al.*, 2010), and Parry Channel (Mudie and Rochon, 2001) highlight the need for more detailed marine studies within the CAA. Additionally, particular attention needs to be directed towards standardized dating and calibration (Coulthard *et al.*, 2010), and the integration of marine and terrestrial records

within the specific context of their physiographic setting (Pieńkowski *et al.*, 2011). In the interim, our study represents the first marine palaeoenvironmental study from Coronation Gulf. Such high-resolution records enable an improved understanding of recent Arctic climate shifts, and allow the placement of Holocene climate into a necessary, broader context.

### Supporting information

Additional supporting information can be found in the online version of this article:

Fig. S1. Photos of selected dinoflagellate cysts and non-pollen palynomorphs from Coronation Gulf core 99LSSL-001.

Table S1. Full list of microfossil taxa (dinocysts and NPPs) present in core 99LSSL-001, with taxonomic designations.

Please note: This supporting information is supplied by the authors, and may be re-organized for online delivery, but is not copy-edited or typeset by Wiley-Blackwell. Technical support issues arising from supporting information (other than missing files) should be addressed to the authors.

**Acknowledgements.** Grateful thanks are extended to Jane Eert (Institute of Ocean Science), for obtaining the boxcore on the Swedish-led Tundra Northwest 99 expedition of the CCGS *Louis S. St-Laurent* through the Northwest Passage. We also appreciate the help of Owen Brown and William LeBlanc (GSCA) in providing grain size and carbon analyses. PJM acknowledges the technical support of S. Blasco's ArcticNet Geohazards Program, and the GSCA Climate Change Program 1999–2004. AJP thanks C. Schweger and H. Friebe (University of Alberta) for the use of the palynology lab and help with sample processing, as well as O. Catuneanu (University of Alberta) for use of microscope facilities. Funding from the NSERC Northern Chair Program (awarded to JE) enabled radiocarbon dating for this project. We thank Jens Matthiessen and one anonymous reviewer whose comments greatly improved the manuscript. We also thank Antony Long for editorial handling of our manuscript.

**Abbreviations.** AMS, accelerator mass spectrometry; CAA, Canadian Arctic Archipelago; IRD, ice-rafted debris; LIA, Little Ice age; MWP, Mediaeval Warm Period; NPP, non-pollen palynomorphs; TC, total carbon; TIC, total organic carbon; TOC, total organic carbon.

### References

- Bassett J, Crompton CW, Parmelee JA. 1978. An atlas of airborne pollen grains and common fungus spores of Canada. *Canadian Department of Agriculture Research Branch Monograph* **18**: 1–321.
- Beaudoin J, Hughes Clarke J, *et al.* 2004. A sound speed decision support system for multibeam sonar operations in the Canadian Arctic. [http://www.omg.unb.ca/omg/papers/beaudoin\\_ASM2004\\_poster.pdf](http://www.omg.unb.ca/omg/papers/beaudoin_ASM2004_poster.pdf) [20 September 2010].
- Belt ST, Vare LL, Massé G, *et al.* 2010. Striking similarities in temporal changes to spring sea ice occurrence across the central Canadian Arctic Archipelago over the last 7000 years. *Quaternary Science Reviews* **29**: 3489–3504.
- Bérard-Therriault L, Poulin M, Bossé L. 1999. *Guide d'identification du phytoplancton marin de l'estuaire et du Golfe du Saint-Laurent incluant également certains protozoaires*. CNRC-NRC: Ottawa.
- Bourgeois JC. 2000. Seasonal and interannual pollen variability in snow layers of arctic ice caps. *Review of Palaeobotany and Palynology* **108**: 17–36.
- Bourgeois JC, Koerner RM, Alt BT. 1985. Airborne pollen, a unique air mass tracer: its influx to the Canadian High Arctic. *Annals of Glaciology* **7**: 109–116.
- Bradley RS. 1990. Holocene paleoclimatology of the Queen Elizabeth Islands, Canadian High Arctic. *Quaternary Science Reviews* **9**: 365–384.
- CAVM Team. 2003. *Circumpolar Arctic vegetation map*. Conservation of Arctic flora and fauna (CAFF) Map No. 1, US Fish and Wildlife Service, scale 1:7,500,000.

- Coulthard RD, Furze MFA, Pieńkowski AJ, *et al.* 2010. New marine  $\Delta R$  values for Arctic Canada. *Quaternary Geochronology* **5**: 419–434.
- Doubleday NC, Smol JP. 2005. Atlas and classification scheme of Arctic combustion particles suitable for paleoenvironmental work. *Journal of Paleolimnology* **33**: 393–431.
- Dowdeswell JA, Whittington RJ, Jennings AE, *et al.* 2000. An origin for laminated glacialine sediments through sea-ice build-up and suppressed iceberg rafting. *Sedimentology* **47**: 557–576.
- Dredge LA. 2001. Where the river meets the sea: geology and landforms of the lower Coppermine river valley and Kugluktuk, Nunavut. *Geological Survey of Canada Miscellaneous Report* **69**: 1–76.
- Dyke AS. 2004. An outline of North American deglaciation with emphasis on central and northern Canada. In *Quaternary glaciations, extent and chronology. Part II. North America. Development in Quaternary Science*, Vol. 2b, Ehlers J, Gibbard PL (eds) Elsevier: Amsterdam; 371–406.
- Dyke AS, Prest V. 1987. Late Wisconsinan and Holocene history of the Laurentide Ice Sheet. *Géographie physique et Quaternaire* **41**: 237–263.
- Dyke AS, Hooper J, Savelle JM. 1996. A history of sea ice in the Canadian Arctic Archipelago based on postglacial remains of the bowhead whale (*Balaena mysticetus*). *Arctic* **49**: 235–255.
- England J. 1987. Glaciation and the evolution of the Canadian high arctic landscape. *Geology* **15**: 419–424.
- England J, Atkinson N, Bednarski J, *et al.* 2006. The Innuitian Ice Sheet: configuration, dynamics and chronology. *Quaternary Science Reviews* **25**: 689–703.
- England J, Furze MFA, Doupé JP. 2009. Revision of the NW Laurentide Ice Sheet: implications for paleoclimate, the northeast extremity of Beringia, and Arctic Ocean sedimentation. *Quaternary Science Reviews* **28**: 1573–1596.
- Environment Canada. 2010a. Canadian climate normals or averages 1971–2000. National Climate Data and Information Archive. [http://www.climate.weatheroffice.gc.ca/climate\\_normals/index\\_e.html](http://www.climate.weatheroffice.gc.ca/climate_normals/index_e.html) [1 September 2010].
- Environment Canada. 2010b. Water Survey of Canada. Archived hydrometric data. [http://www.wsc.ec.gc.ca/hydat/H2O/index\\_e.cfm?cname=main\\_e.cfm](http://www.wsc.ec.gc.ca/hydat/H2O/index_e.cfm?cname=main_e.cfm) [1 September 2010].
- Fortin M-C, Gajewski K. 2010. Holocene climate change and its effect on lake ecosystem production on Northern Victoria Island, Canadian Arctic. *Journal of Paleolimnology* **43**: 219–234.
- Gajewski K, Atkinson DA. 2003. Climatic change in northern Canada. *Environmental Review* **11**: 69–102.
- Gregory TR, Smart CW, Hart MB, *et al.* 2010. Holocene palaeoceanographic changes in Barrow Strait, Canadian Arctic: foraminiferal evidence. *Journal of Quaternary Science* **25**: 903–910.
- Grumet NS, Wake CF, Mayewski PA, *et al.* 2001. Variability of sea-ice extent in Baffin Bay over the last millennium. *Climatic Change* **49**: 129–145.
- Head MJ, Harland R, Rochon A. 2001. Cold marine indicators of the late Quaternary: the new dinoflagellate cyst genus *Islandinium* and related morphotypes. *Journal of Quaternary Science* **16**: 621–636.
- Headland RK. 2010. Ten decades of transits of the Northwest Passage. *Polar Geography* **33**: 1–13.
- Houston S, Ball T, Houston M. 2003. *Eighteenth-Century Naturalists of Hudson Bay*. McGill-Queen's University Press: Montreal.
- Howell SEL, Tivy A, Yackel JJ, *et al.* 2008. Multi-year sea-ice conditions in the western Canadian Arctic Archipelago Region of the Northwest Passage: 1968–2006. *Atmosphere–Ocean* **46**: 229–242.
- Hunt AS, Corliss BH. 1993. Distribution and microhabitats of living (stained) benthic foraminifera from the Canadian Arctic Archipelago. *Marine Micropaleontology* **20**: 321–345.
- Ingram RG, Prinsenberg S. 1998. Coastal oceanography of Hudson Bay and surrounding eastern Canadian Arctic waters. In *The sea. Vol. 11: The Global Coastal Ocean, Regional Studies and Syntheses*, Robinson AR, Brink KH (eds) Wiley: New York; 835–862.
- Jakobsson M, Macnab R, Mayer L, *et al.* 2008. An improved bathymetric portrayal of the Arctic Ocean: implications for ocean modelling and geological, geophysical and oceanographic analyses. *Geophysical Research Letters* **35**: L07602.
- Juggins S. 2007. *C2 Version 1.5 User Guide: Software for Ecological and Palaeoecological Data Analysis and Visualisation*. Newcastle University: Newcastle upon Tyne.
- Keigwin LD, Pickart RS. 1999. Slope water current over the Laurentian Fan on interannual to millennial time scales. *Science* **286**: 520–523.
- Keigwin LD, Sachs JP, Rosenthal Y. 2003. A 1600-year history of the Labrador current off Nova Scotia. *Climate Dynamics* **21**: 53–62.
- Kerr DE, Dredge LA, Ward BC. 1997. *Surficial geology, Coppermine (east half), District of Mackenzie, Northwest Territories*. Geological Survey of Canada Map 1910A, scale 1:125 000.
- Knudsen KL, Eiriksson J, Jansen E, *et al.* 2004. Palaeoceanographic changes off North Iceland through the last 1200 years: foraminifera, stable isotopes, diatoms and ice-rafted debris. *Quaternary Science Reviews* **23**: 2231–2246.
- Knudsen KL, Stabell B, Seidenkrantz M-S, *et al.* 2008. Deglacial and Holocene conditions in northernmost Baffin Bay: sediments, foraminifera, diatoms and stable isotopes. *Boreas* **37**: 346–376.
- Koerner RM. 1977. Devon Island Ice Cap: core stratigraphy and paleoclimate. *Science* **196**: 15–18.
- Koerner RM, Fisher DA. 1990. A record of Holocene summer climate from a Canadian high-Arctic ice core. *Nature* **343**: 630–631.
- Koerner RM, Paterson WSB. 1974. Analysis of a core through the Meighen Ice Cap, Arctic Canada and its paleoclimatic implications. *Quaternary Research* **4**: 253–263.
- Kunz-Pirrung M. 1998. Rekonstruktion der Oberflächenmassen in der östlichen Laptevsee im Holozän anhand von aquatischen Palynomorphen. *Berichte zur Polarforschung* **281**: 1–117.
- Lamoureux SF, England JH, Sharp MJ, *et al.* 2001. A varve record of increased 'Little Ice Age' rainfall associated with volcanic activity, Arctic Archipelago, Canada. *The Holocene* **11**: 243–249.
- LeBlanc M, Gajewski K, Hamilton P. 2004. A diatom-based Holocene paleoenvironmental record from a lake on the Boothia Peninsula, Nunavut, Canada. *The Holocene* **14**: 423–431.
- Ledu D, Rochon A, de Vernal A, *et al.* 2008. Palynological evidence of Holocene climate change in the eastern Arctic: a possible shift in the Arctic oscillation at the millennial time scale. *Canadian Journal of Earth Sciences* **45**: 1363–1375.
- Ledu D, Rochon A, de Vernal A, *et al.* 2010a. Holocene sea ice history and climate variability along the main axis of the Northwest Passage, Canadian Arctic. *Paleoceanography* **25**: PA2213.
- Ledu D, Rochon A, de Vernal A, *et al.* 2010b. Holocene paleoceanography of the northwest passage, Canadian Arctic Archipelago. *Quaternary Science Reviews* **29**: 3468–3488.
- Levac E, de Vernal A, Blake W Jr. 2001. Sea-surface conditions in northernmost Baffin Bay during the Holocene: palynological evidence. *Journal of Quaternary Science* **16**: 353–363.
- Maasch KA, Mayewski PA, Rohling EJ, *et al.* 2005. A 2000 year context for modern climate change. *Geografiska Annaler* **87A**: 7–15.
- MacDonald GM, Porinchu DF, Rolland N, *et al.* 2009. Paleolimnological evidence of the response of the central Canadian treeline zone to radiative forcing and hemispheric patterns of temperature change over the past 2000 years. *Journal of Paleolimnology* **41**: 129–141.
- Macko SJ, Segall MP, Pereira CPG. 1985. *Geochemical and mineralogical studies in the Arctic Archipelago. Report 095c.23420-5-M744*. Centre for Cold Ocean Resources Engineering (C-CORE): Memorial University of Newfoundland: St John's.
- MacLean B, Sonnichsen G, Vilks G, *et al.* 1989. Marine geological and geotechnical investigations in Wellington, Byam Martin, Austin, and adjacent channels, Canadian Arctic Archipelago. *Geological Survey of Canada Paper* **89-11**: 1–69.
- Mann ME, Zhang Z, Rutherford S, *et al.* 2009. Global signatures and dynamical origins of the Little Ice Age and Medieval Climate Anomaly. *Science* **326**: 1256–1260.
- Marret F, Zonneveld KAF. 2003. Atlas of modern organic-walled dinoflagellate cyst distribution. *Review of Paleobotany and Palynology* **125**: 1–200.
- Matsuoka K, Kawami H, Nagai S, *et al.* 2009. Re-examination of cyst-motile relationships of *Polykrikos kofoidii* Chatton and *Polykrikos schwartzii* Bütschli (Gymnodiniales, Dinophyceae). *Review of Paleobotany and Palynology* **154**: 79–90.
- Matthiessen J, Kunz-Pirrung M, Mudie PJ. 2000. Freshwater chlorophycean algae in recent marine sediments of the Beaufort, Laptev and Kara seas (Arctic Ocean) as indicators of river runoff. *International Journal of Earth Sciences* **89**: 470–485.

- Matthiessen J, de Vernal A, Head M, *et al.* 2005. Modern organic-walled dinoflagellate cysts and their (paleo-) environmental significance. *Paläontologische Zeitschrift* **79**: 3–51.
- Maxwell JB. 1981. Climatic regions of the Canadian Arctic islands. *Arctic* **34**: 225–240.
- McAndrews JH, Berti AA, Norris G. 1973. *Key to the Quaternary Pollen and Spores of the Great Lakes Region*. Royal Ontario Museum: Toronto.
- McLaughlin F, Carmack E, O'Brien M, *et al.* 2009. Physical and chemical data from the Canadian Arctic Archipelago, August 23 to September 8, 1999. *Canadian Data Report of Hydrography and Ocean Sciences* **179**: 1–140.
- Mudie PJ. 1982. Pollen distribution in recent marine sediments. *Canadian Journal of Earth Sciences* **19**: 729–747.
- Mudie PJ. 1992. Circum-Arctic Quaternary and Neogene marine palynofloras: paleoecology and statistical analysis. In *Neogene and Quaternary Dinoflagellate Cysts and Acritarchs*, Head MJ, Wrenn JH (eds) American Association of Stratigraphic Palynologists: Foundation: Dallas, TX; 347–390.
- Mudie PJ, Harland R. 1996. Aquatic Quaternary. In *Palynology: Principles and Applications*, Jansonius J, McGregor DC (eds) American Association of Stratigraphic Palynologists: Foundation: Dallas, TX; 843–877.
- Mudie PJ, Rochon A. 2001. Distribution of dinoflagellate cysts in the Canadian Arctic marine region. *Journal of Quaternary Science* **16**: 595–602.
- Mudie PJ, Short SK. 1985. Marine palynology of Baffin Bay. In *Quaternary Environments: Eastern Canadian Arctic, Baffin Bay and West Greenland*, Andrews JT (ed.). George Allen & Unwin: London; 263–308.
- Mudie PJ, Rochon A, Levac E. 2005. Decadal-scale sea ice changes in the Canadian Arctic and their impacts on humans during the past 4,000 years. *Environmental Archeology* **10**: 113–126.
- Mudie PJ, Rochon A, Prins MA, *et al.* 2006. Late Pleistocene–Holocene marine geology of Nares Strait region: palaeoceanography from foraminifera and dinoflagellate cysts, sedimentology and stable isotopes. *Polarforschung* **74**: 169–183.
- Mudie PJ, Leroy SAG, Marret F, *et al.* 2011. Non-pollen palynomorphs (NPP): indicators of salinity and environmental change in the Caspian–Black Sea–Mediterranean Corridor. In *Geology and Geoarchaeology of the Black Sea Region: Beyond the Flood Hypothesis*, Buynevich I, Yanko-Hombach V, Smyntyna O, Martin R, Siegel D (eds) *Geological Society of America Special Paper* **473**: 89–115.
- Nichols H. 1975. Palynological and paleoclimatic study of the Late Quaternary displacement of the boreal forest–tundra ecotone in Keewatin and Mackenzie, N.W.T., Canada. *Institute of Arctic and Alpine Research Occasional Paper* **15**: 1–87.
- Noorany I. 1984. Phase relations in marine soils. *Journal of the Geotechnical Engineering Division* **110**: 539–543.
- Ó Cofaigh C, Dowdeswell JA. 2001. Laminated sediments in glaci-marine environments: diagnostic criteria for their interpretation. *Quaternary Science Reviews* **20**: 1411–1436.
- Osborn TJ, Briiffa KR. 2006. The spatial extent of 20th century warmth in the context of the past 1200 years. *Science* **311**: 841–844.
- Overpeck J, Hughen K, Hardy D, *et al.* 1997. Arctic environmental change of the last four centuries. *Science* **278**: 1251–1256.
- Paul CA, Rühland KM, Smol JP. 2010. Diatom-inferred climatic and environmental changes over the last ~9000 years from a low Arctic (Nunavut, Canada) tundra lake. *Palaeogeography, Palaeoclimatology, Palaeoecology* **291**: 205–216.
- Peros MC, Gajewski K. 2008. Holocene climate and vegetation change on Victoria Island, western Canadian Arctic. *Quaternary Science Reviews* **27**: 235–249.
- Peros MC, Gajewski K. 2009. Pollen-based reconstructions of late Holocene climate from the central and western Canadian Arctic. *Journal of Paleolimnology* **41**: 161–175.
- Pfirman S, Gascarde J-C, Wollenberg I, *et al.* 1989. Particle-laden Eurasian Arctic sea ice: observations from July and August 1987. *Polar Research* **7**: 59–66.
- Pharand D. 1984. *The Northwest Passage: Arctic straits*. Martinus Nijhoff: Dordrecht.
- Pieńkowski AJ, England JH, Furze MFA, *et al.* 2011. The deglacial to postglacial marine environments of Barrow Strait, Canadian Arctic Archipelago. *Boreas* [doi: 10.1111/j.1502-3885.2011.00227.x]
- Podritske B, Gajewski K. 2007. Diatom community response to multiple scales of Holocene climate variability in a small lake on Victoria Island, NWT, Canada. *Quaternary Science Reviews* **26**: 3179–3196.
- Porinchu DF, MacDonald GM, Rolland N. 2009. A 2000 year midge-based paleotemperature reconstruction from the Canadian Arctic archipelago. *Journal of Paleolimnology* **41**: 177–188.
- Pospelova V, Chmura GL, Walker HA. 2004. Environmental factors influencing the spatial distribution of dinoflagellate cyst assemblages in shallow lagoons of southern New England (USA). *Review of Palaeobotany and Palynology* **128**: 7–34.
- Pospelova V, Chmura GL, Boothman WS, *et al.* 2005. Spatial distribution of modern dinoflagellate cysts in polluted estuarine sediments from Buzzards Bay (Massachusetts, USA) embayments. *Marine Ecology Progress Series* **292**: 23–40.
- Prest VK, Grant DR, Rampton V. 1968. *Glacial Map of Canada*. Geological Survey of Canada Map 1253A, scale 1:5 000 000.
- Przybylak R, Vizi Z. 2005. Air temperature changes in the Canadian Arctic from the early instrumental period to modern times. *International Journal of Climatology* **25**: 1507–1522.
- Reid PC, John AWG. 1978. Tintinnid cysts. *Journal of the Marine Biological Association UK* **58**: 551–557.
- Reimer PJ, Baillie MGL, Bard E, *et al.* 2009. IntCal09 and Marine09 radiocarbon age calibration curves, 0–50,000 years cal BP. *Radiocarbon* **51**: 1111–1150.
- Richerol T, Rochon A, Blasco S, *et al.* 2008a. Distribution of dinoflagellate cysts in surface sediments of the Mackenzie Shelf and Amundsen Gulf, Beaufort Sea (Canada). *Journal of Marine Systems* **74**: 825–863.
- Richerol T, Rochon A, Blasco S, *et al.* 2008b. Evolution of paleo-sea-surface conditions over the last 600 years in the Mackenzie Trough, Beaufort Sea (Canada). *Marine Micropaleontology* **68**: 6–20.
- Rochon A, de Vernal A, Turon J-L, *et al.* 1999. *Distribution of Recent Dinoflagellate Cysts in Surface Sediments from the North Atlantic Ocean and Adjacent Seas in Relation to Sea-Surface Parameters*. American Association of Stratigraphic Palynologists: Foundation: Dallas, TX.
- Roncaglia L. 2004. New acritarch species from Holocene sediments in central West Greenland. *Grana* **43**: 1–88.
- Roncaglia L, Kuijpers A. 2004. Palynofacies and dinoflagellate cysts from Igaliku Fjord, Greenland. *The Holocene* **14**: 172–184.
- Rühland K, Smol JP. 2005. Diatom shifts as evidence for recent sub-arctic warming in a remote tundra lake, NWT, Canada. *Palaeogeography, Palaeoclimatology, Palaeoecology* **226**: 1–16.
- Schell TM, Moss TJ, Scott DB, *et al.* 2008. Paleo-sea ice conditions of the Amundsen Gulf, Canadian Arctic Archipelago: implications from the foraminiferal record of the last 200 years. *Journal of Geophysical Research* **113**: C03S02.
- Schröder-Adams CJ, Cole FE, Medioli FS, *et al.* 1990. Recent Arctic shelf foraminifera: seasonally ice covered vs. perennially ice covered areas. *Journal of Foraminiferal Research* **20**: 8–36.
- Scott DB, Mudie PJ, Vilks G, *et al.* 1984. Latest Pleistocene–Holocene paleoceanographic trends on the continental margin of eastern Canada: foraminiferal, dinoflagellate, and pollen evidence. *Marine Micropaleontology* **9**: 181–218.
- Scott DB, Schell T, St-Onge G, *et al.* 2009. Foraminiferal assemblage changes over the last 15,000 years on the Mackenzie–Beaufort Sea Slope and Amundsen Gulf, Canada: implications for past sea ice conditions. *Paleoceanography* **24**: PA2219.
- Seidenkrantz M-S, Roncaglia L, Fischel A, *et al.* 2008. Variable North Atlantic climate seesaw patterns documented by a late Holocene marine record from Disko Bugt, West Greenland. *Marine Micropaleontology* **68**: 66–83.
- Sharpe DR. 1992. Quaternary geology of Wollaston Peninsula, Victoria Island, Northwest Territories. *Geological Survey of Canada Memoir* **434**: 1–84.
- Smith JN. 2001. Why should we believe <sup>210</sup>Pb geochronologies? *Journal of Environmental Radioactivity* **55**: 121–123.

- Smith JN, Walton A. 1980. Sediment accumulation rates and geochronologies measured in the Saguenay Fjord using the Pb-210 dating method. *Geochimica et Cosmochimica Acta* **44**: 225–240.
- Smith JN, Lee K, Gobeil C, et al. 2009. Natural rates of sediment containment of PAH, PCB and metal inventories in Sydney Harbour, Nova Scotia. *Science of the Total Environment* **407**: 4858–4869.
- Smol JP, Wolfe AP, Birks HJB, et al. 2005. Climate-driven regime shifts in the biological communities of arctic lakes. *Proceedings of the National Academy of Sciences of the USA* **102**: 4397–4402.
- Solomon S, Qin D, Manning M, et al. (eds) 2007. *Climate Change 2007: The Physical Science Basis. Contribution of Working Group I to the Fourth Assessment Report of the Intergovernmental Panel on Climate Change*. Cambridge University Press: Cambridge, UK.
- Stancliffe RPW. 1991. Microforaminiferal linings. In *Palynology: Principles and Applications*, Jansonius J, McGregor DC (eds) American Association of Stratigraphic Palynologists: Foundation: Dallas, TX; 373–379.
- Stewart EJ, Howell SEL, Draper D, et al. 2007. Sea ice in Canada's Arctic: implications for cruise tourism. *Arctic* **60**: 370–380.
- Strelis I, Kennedy RW. 1967. *Identification of North American Commercial Pulpwoods and Pulp Fibres*. University of Toronto Press: Toronto; 1–117.
- Stuiver M, Reimer PJ, Reimer RW. 2010. CALIB 6.0 (WWW program and documentation).
- Thorsteinsson R, Tozer ET. 1962. Banks, Victoria, and Stefansson Islands, Arctic Archipelago. *Geological Survey of Canada Memoir* **330**: 1–85.
- Turner J, Overland JE, Walsh JE. 2007. An Arctic and Antarctic perspective on recent climate change. *International Journal of Climatology* **27**: 277–293.
- Vare LL, Massé G, Gregory TR, et al. 2009. Sea ice variations in the central Canadian Arctic Archipelago during the Holocene. *Quaternary Science Reviews* **28**: 1354–1366.
- Vilks G. 1969. Recent foraminifera in the Canadian Arctic. *Micropaleontology* **15**: 35–60.
- Wang J, Cota GF, Comiso JC. 2005. Phytoplankton in the Beaufort and Chukchi seas: distribution, dynamics, and environmental forcing. *Deep-Sea Research II* **52**: 3355–3368.
- Wolken GJ, England JH, Dyke AS. 2005. Changes in late-Neoglacial perennial snow/ice extent and equilibrium-line altitudes in the Queen Elizabeth Islands, Arctic Canada. *The Holocene* **18**: 615–627.
- Zabenskie S, Gajewski K. 2007. Post-glacial climatic change on Boothia Peninsula, Nunavut, Canada. *Quaternary Research* **68**: 261–270.